THE JOURNAL OF BIOLOGICAL CHEMISTRY VOL. 291, NO. 34, pp. 17787–17803, August 19, 2016

Small Molecule Inhibitors Targeting Tec Kinase Block Unconventional Secretion of Fibroblast Growth Factor 2*

Received for publication, March 25, 2016, and in revised form, June 24, 2016 Published, JBC Papers in Press, July 5, 2016, DOI 10.1074/jbc.M116.729384

Giuseppe La Venuta[‡], Sabine Wegehingel[‡], Peter Sehr[§], Hans-Michael Müller[‡], Eleni Dimou[‡], Julia P. Steringer[‡], Mareike Grotwinkel[‡], Nikolai Hentze[¶], Matthias P. Mayer[¶], David W. Will[§], Ulrike Uhrig[§], Joe D. Lewis[§], and Walter Nickel[‡1]

From the [‡]Heidelberg University Biochemistry Center (BZH), Im Neuenheimer Feld 328, 69120 Heidelberg, Germany, the [§]European Molecular Biology Laboratory (EMBL), Meyerhofstrasse 1, 69117 Heidelberg, Germany, and the [¶]Zentrum für Molekulare Biologie der Universität Heidelberg (ZMBH), DKFZ-ZMBH Allianz, Im Neuenheimer Feld 282, 69120 Heidelberg, Germany

Fibroblast growth factor 2 (FGF2) is a potent mitogen promoting both tumor cell survival and tumor-induced angiogenesis. It is secreted by an unconventional secretory mechanism that is based upon direct translocation across the plasma membrane. Key steps of this process are (i) phosphoinositide-dependent membrane recruitment, (ii) FGF2 oligomerization and membrane pore formation, and (iii) extracellular trapping mediated by membrane-proximal heparan sulfate proteoglycans. Efficient secretion of FGF2 is supported by Tec kinase that stimulates membrane pore formation based upon tyrosine phosphorylation of FGF2. Here, we report the biochemical characterization of the direct interaction between FGF2 and Tec kinase as well as the identification of small molecules that inhibit (i) the interaction of FGF2 with Tec, (ii) tyrosine phosphorylation of FGF2 mediated by Tec *in vitro* and in a cellular context, and (iii) unconventional secretion of FGF2 from cells. We further demonstrate the specificity of these inhibitors for FGF2 because tyrosine phosphorylation of a different substrate of Tec is unaffected in their presence. Building on previous evidence using RNA interference, the identified compounds corroborate the role of Tec kinase in unconventional secretion of FGF2. In addition, they are valuable lead compounds with great potential for drug development aiming at the inhibition of FGF2-dependent tumor growth and metastasis.

Although the majority of secretory proteins carry signal peptides for endoplasmic reticulum/Golgi-dependent secretion, a set of important growth factors and cytokines involved in tumor-induced angiogenesis and inflammatory responses makes use of alternative routes. These processes have collectively been termed "unconventional protein secretion" (1–5). FGF2 and IL1β are prominent examples for secretory proteins that make use of such pathways (4–12). The molecular mechanism by which IL1β is secreted from cells is debated and may differ in some aspects between various kinds of immune cells (4, 5, 10, 13–16). By contrast, the mechanism of the unconventional secretory pathway of FGF2 is emerging with great molecular detail (12). It is based upon direct translocation of folded species of FGF2 across plasma membranes (9, 17–20). Hallmarks of this process are (i) FGF2 recruitment at the inner leaflet of the plasma membrane mediated by the phosphoinositide $PI(4,5)P_2$[2] (9, 21, 22), (ii) FGF2 oligomerization and membrane pore formation (11, 12, 23, 24), and (iii) extracellular trapping of FGF2 mediated by membrane-proximal heparan sulfate proteoglycans (1, 2, 25, 26). Recently, these hallmarks of FGF2 secretion have also been implicated in unconventional secretion of HIV-Tat (HIV trans-activator of transcription) (12, 27–30). Based on a genome-wide RNAi screening approach, two additional factors physically associated with the plasma membrane have been identified to play a role in FGF2 secretion, Tec kinase (9, 11, 12, 24, 31) and ATP1A1 (12, 32–34), the α subunit of the Na/K-ATPase (35). Although the precise role of ATP1A1 in FGF2 membrane translocation into the extracellular space is unknown, Tec kinase was shown to directly interact with FGF2, resulting in phosphorylation of tyrosine 81 (9, 31). It was further shown that a phosphomimetic variant form of FGF2 is secreted from cells in a Tec kinase-independent manner (9, 31). Furthermore, based upon biochemical reconstitution experiments, a phosphomimetic form of FGF2 was found to be characterized by an increased ability to form $PI(4,5)P_2$-dependent membrane pores (23, 24), the intermediates of FGF2 membrane translocation in cells (12).

Tec kinase contains a N-terminal pleckstrin homology (PH) domain mediating recruitment at the inner leaflet of plasma membranes in a $PI(3,4,5)P_3$-dependent manner. In a number of physiological settings, activation of various kinds of receptors causes $PI(3,4,5)P_3$ levels to increase (36, 37). Under these conditions, Tec kinases are recruited to the inner leaflet of the plasma membrane (38). Tec kinase then becomes phosphorylated by plasma membrane-resident Src kinases or by autophosphorylation within its activation loop resulting in enzymatic

* This work was supported by the Baden-Württemberg Stiftung (Stuttgart, Germany). In addition, funds were received from the German Research Council (DFG-SFB 638, DFG-SFB/TRR 186, DFG-SFB/TRR 83, DFG Ni 423/6-1, and DFG Ni 423/7-1), the AID-NET program of the Federal Ministry for Education and Research of Germany, and the DFG Cluster of Excellence, CellNetworks. The authors declare that they have no conflicts of interest with the contents of this article.

[1] To whom correspondence should be addressed: Heidelberg University Biochemistry Center (BZH), Im Neuenheimer Feld 328, 69120 Heidelberg, Germany. Tel.: 49-6221-545425; Fax: 49-6221-544366; E-mail: walter.nickel@bzh.uni-heidelberg.de.

[2] The abbreviations used are: $PI(4,5)P_2$, phosphatidylinositol 4,5-bisphosphate; $PI(3,4,5)P_3$, phosphatidylinositol 3,4,5-trisphosphate; CARP, cardiac adriamycin-responsive protein; MBP, maltose-binding protein; PH, pleckstrin homology; SH1, SH2, and SH3, Src homology 1, 2, and 3, respectively; TH, Tec homology; Ni-NTA, nickel-nitrilotriacetic acid; BisTris, 2-[bis(2-hydroxyethyl)amino]-2-(hydroxymethyl)propane-1,3-diol.

activation (39). In its activated state, Tec kinase phosphorylates target proteins (36). Because FGF2 is a key signaling molecule in the context of many cancers, Tec kinase-regulated secretion of FGF2 represents an interesting link to the up-regulation of PI3Ks in many tumor cells (40). PI3Ks catalyze the formation of $PI(3,4,5)P_3$, and high cellular levels of this phosphoinositide are likely to support efficient secretion of FGF2, which, in turn, promotes tumor cell proliferation and tumor-induced angiogenesis.

Based on these considerations, the current study aimed at the identification of small molecules that block the function of Tec kinase in the unconventional secretory pathway of FGF2. Following the determination of affinity between FGF2 and Tec kinase, an Alpha® protein-protein interaction assay (34) was used to screen a library of 79,000 compounds to identify small molecules inhibitors that block binding of FGF2 to Tec kinase. Here we report the structure of three active, structurally related compounds that (i) block the interaction of FGF2 with Tec kinase, (ii) prevent phosphorylation of FGF2 by Tec kinase *in vitro* and in a cellular context, and (iii) inhibit unconventional secretion of FGF2 from cells. Based upon two inactive derivatives of these inhibitors, a highly specific mode of action of the active compounds was established. All three active compounds were found to efficiently inhibit binding of FGF2 to Tec kinase with IC_{50} values in the low micromolar range. By contrast, pleiotropic effects on general cell viability were not observed. In terms of the mechanism of inhibition, the active compounds appear to block Tec kinase autoactivation in the absence of a bound substrate. Because FGF2 cannot bind to Tec in the presence of the active compounds, tyrosine phosphorylation of FGF2 is prevented. By contrast, tyrosine phosphorylation of another substrate of Tec kinase, STAP1 (signal-transducing adaptor protein 1), remained unaffected in the presence of the active compounds. These experiments establish a high degree of specificity of the reported compounds selectively blocking FGF2 as a substrate of Tec kinase. The potential of the reported small molecule inhibitors as lead compounds for drug development is discussed, in particular with regard to tumor-induced angiogenesis (41, 42) and the role of FGF2 as a tumor cell survival factor (43–46).

Results

Biochemical Characterization of FGF2 Binding to Tec Kinase—A first set of experiments was based on biochemical pull-down experiments to probe for a direct interaction between FGF2 and Tec kinase as well as to define the domain in Tec kinase that binds to FGF2. FGF2 was expressed in *Escherichia coli*, purified to homogeneity (23, 24), and covalently coupled to epoxy beads (34). Various constructs of Tec kinase were expressed and purified from insect cells (Fig. 1*A*). These experiments revealed that the kinase domain (SH1) of Tec is sufficient for binding to FGF2 (Fig. 1*B*). Consistently, a construct containing the SH1, SH2, and SH3 domains of Tec (GST-NΔ173 Tec) did bind to FGF2 as well (Fig. 1*B*). By contrast, constructs restricted to either the PH and Tec homology (TH) domains (GST-PH-TH), the SH3/SH2 domains (GST-SH3-SH2), or GST alone did not bind to FGF2 (Fig. 1*B*). The Coomassie-stained gel shown in Fig. 1*B* was quantified using the LI-COR imaging system (Fig. 1*C*).

To determine affinity between FGF2 and Tec kinase, steady-state fluorescence polarization experiments were conducted. FGF2 was fluorescently labeled as explained under "Experimental Procedures," and binding experiments with various Tec constructs were performed in solution (Fig. 2*A*). Similar to the results shown in Fig. 1, a direct interaction of FGF2 with both the SH1 kinase domain of Tec and GST-NΔ173 Tec was observed. The significance of these findings was confirmed by competition experiments using unlabeled FGF2. In the presence of 50 μM unlabeled FGF2, the interaction of labeled FGF2 with both the kinase domain (SH1) of Tec (Fig. 2*B*) and GST-NΔ173 Tec (Fig. 2*C*) was blocked. By contrast, FGF2 did not bind to GST-PH-TH, GST-SH3-SH2, or GST alone (Fig. 2*A*). To determine the affinity between FGF2 and Tec kinase, fluorescently labeled FGF2 (50 nM) was incubated with increasing concentrations (0.078–20 μM) of the various Tec constructs indicated (Fig. 2*A*). Data points were fitted, and dissociation constants were calculated as explained under "Experimental Procedures." Dissociation constants of 1.434 μM ± 0.55 (S.E.) and 1.032 μM ± 0.29 (S.E.) were obtained for GST-NΔ173 Tec and the kinase domain (SH1) of Tec, respectively.

Large Scale Small Molecule Screening for Inhibitors That Block Binding of FGF2 to Tec Kinase—To identify small molecule inhibitors that prevent the interaction between FGF2 and Tec kinase, a screening assay was established based upon Alpha® technology (47). His-tagged FGF2 and GST-tagged NΔ173 Tec were used with glutathione donor and Ni-NTA acceptor beads, respectively. In a cross-titration experiment, suitable protein concentrations of FGF2 and NΔ173 Tec (see "Experimental Procedures") were identified, providing a satisfying signal/noise ratio. Using these conditions, affinity between FGF2 and NΔ173 Tec was analyzed in a competition experiment. Based upon a titration curve with an untagged variant form of FGF2, NΔ25FGF2, a dissociation constant of 0.63 ± 0.03 μM (S.E.) was determined (Fig. 3). When analyzing an unrelated pair of interacting proteins, GST-Titin and His-tagged MBP-CARP, NΔ25FGF2 did not affect the Alpha® signal (Fig. 3). These findings establish a specific and direct interaction between FGF2 and NΔ173 Tec with a dissociation constant comparable with the results obtained in steady-state fluorescence polarization experiments (Fig. 2).

To identify small molecule inhibitors of the interaction between FGF2 and NΔ173 Tec, a small molecule compound library was screened using the AlphaScreen® protein-protein interaction assay described in the legend to Fig. 3. This scaffold-based collection comprises 79,000 compounds. The screening assay was performed at a final compound concentration of 40 μM and revealed 661 compounds that inhibit the interaction between FGF2 and NΔ173 Tec by >40%. The Titin/CARP assay described in the legend to Fig. 3 was used to deselect unspecific compounds. In addition, compounds that were found active toward other targets in previous screening campaigns based on Alpha® technology were deselected. This procedure resulted in a preliminary hit list of 141 compounds inhibiting the interaction between FGF2 and NΔ173 Tec. These compounds were reordered and tested in dose-response exper-

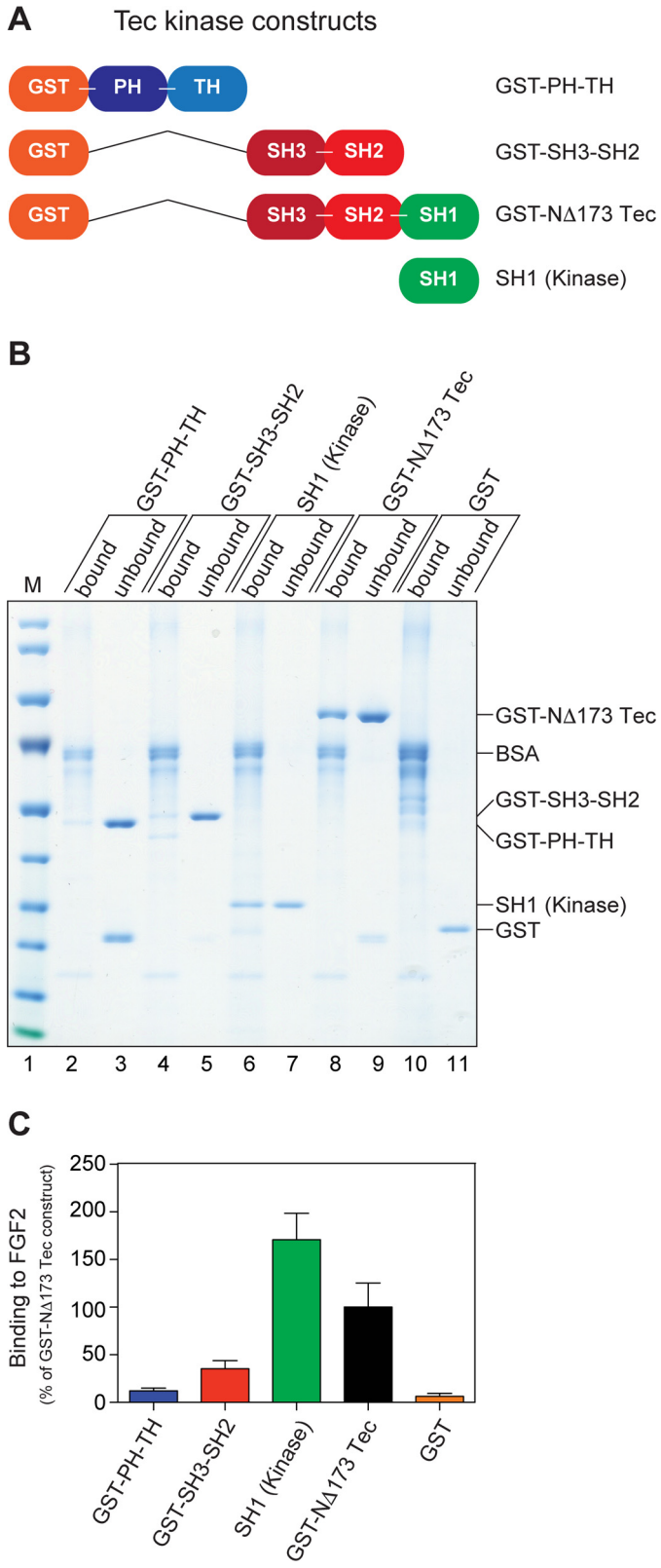

FIGURE 1. **The catalytic SH1 domain of Tec kinase directly interacts with FGF2 as analyzed by biochemical pull-down experiments.** *A*, schematic depiction of the domain structure of Tec constructs used in this study. *B*, pull-down experiments using recombinant FGF2 covalently coupled to epoxy beads as analyzed by SDS-PAGE and Coomassie protein staining. FGF2-conjugated epoxy beads were incubated with each of the four Tec kinase-derived constructs, GST-PH-TH (47.2 kDa; *lanes 2* and *3*), GST-SH3-SH2 (47.9 kDa; *lanes 4* and *5*), SH1 (32.9 kDa; *lanes 6* and *7*), and GST-NΔ173 Tec (80.2 kDa; *lanes 8* and *9*). Because all constructs were used as GST fusion proteins (with the exception of the SH1 kinase domain), binding of GST alone (26.5 kDa; *lanes 10* and *11*) to FGF2-conjugated epoxy beads was taken as a negative control. For each construct, bound (100%) and unbound (1%) fractions were loaded. *Lane 1*, molecular mass markers (*M*; PageRuler prestained protein ladder: 140, 115, 80, 65, 50, 40, 30, 25, 15, and 10 kDa). The gel shown is representative of five independent experiments. *C*, quantification of FGF2 binding to the various Tec constructs depicted in *A*. Coomassie-stained SDS gels were analyzed using the LI-COR Biosciences Odyssey infrared imaging system. The intensity of each band was quantified using Image Studio software (version 2.1.10). For each construct, binding efficiency was calculated relative to unbound material. A comparison of all constructs was conducted, defining FGF2 binding efficiency toward GST-NΔ173 Tec as 100%. The statistical analysis was based upon five independent experiments. *Error bars*, S.D.

iments to determine IC_{50} values, both for the FGF2/Tec validation assay and the Titin/CARP deselection assay (Fig. 3). A set of 28 compounds was found to be characterized by IC50 values of <100 μM. Based upon (i) inhibitory strength in the primary screening assay, (ii) lack of activity in the Titin/CARP deselection assay, and (iii) inhibitory potency in *in vitro* phosphorylation experiments (see Figs. 6 and 7), a final set of three highly active compounds (compounds 6, 14, and 21) was identified (Fig. 4) (58). In addition, two structurally related but inactive compounds (compounds 18 and 19) were selected as controls for all subsequent experiments. With regard to chemical identities, compounds 6, 14, and 19 are based on a 4*H*-pyrido[1,2-*a*]pyrimidin-4-one scaffold. Compounds 6 and 14 have a 2-hydroxymethyl substituent that is condensed to a substituted pyrrole carboxylic acid moiety via an ester function. This ester linkage is potentially metabolically labile *in vivo* due to cleavage by esterases. In addition, compound 6 contains a methyl ester on the pyrrole moiety that is likely to be cleaved *in vivo*. Compound 19 is a more stable analogue of compound 14 that replaces the ester linkage with a much more metabolically stable amide moiety. However, this appears to abolish all activity, although the absence of the bromo substituent in compound 19 makes a definitive conclusion regarding the importance of the linker difficult. It is clear, however, that the 1-(2,4-dimethyl-1H-pyrrol-3-yl)ethanone moiety alone is not sufficient for activity because it is found both in active compound 14 and inactive compound 19. Compound 21 has an alternative 3H-imidazo[4,5-b]pyridine scaffold and contains the 1-(2,4-dimethyl-1H-pyrrol-3-yl)ethanone moiety also found in compounds 14 and 19. The imidazo-pyridine scaffold of compound 21 is partially isosteric to the pyrido-pyrimidone scaffold of compound 14, and indeed this compound retains activity. In addition, the ester linkage is replaced by a sulfanyl-acetyl type link. This indicates that the labile ester linkage found in compounds 6 and 14 can be replaced with more metabolically stable alternatives. Compound 18 has a [1,2,4]triazolo[1,5-a]pyrimidine scaffold, which is also partially isosteric to the pyrido-pyrimidone scaffold of compound 14. Instead of the pyrrole substituent present in all other compounds, it contains a coumarin moiety. The simultaneous modification of both termini of the molecule plus a different amide linker makes this compound rather different from the other active compounds, and it can be considered as a negative control compound.

Determination of IC_{50} Values of Active Compounds—In addition to dose-response experiments that were conducted under screening conditions (see above), we carefully analyzed the

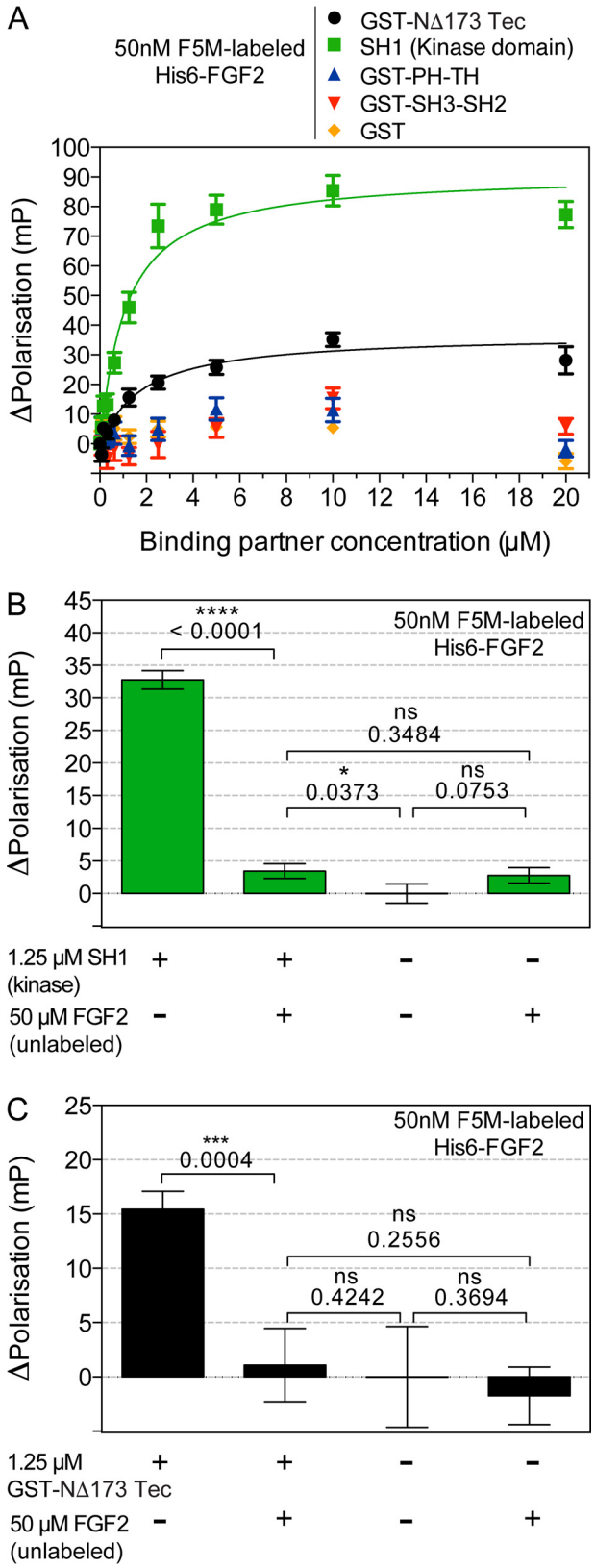

FIGURE 2. **Determination of the dissociation constant of the interaction between FGF2 and various forms of Tec kinase based upon fluorescence polarization.** *A*, fluorescence polarization experiments were conducted using fluorescein-labeled FGF2. FGF2 (at a constant concentration of 50 nM) was incubated with increasing concentrations (0–20 μM) of the various Tec constructs indicated. Following incubation for 3 h at room temperature, changes in polarization (Δ*Polarisation*) (in millipolarization units (*mP*)) were recorded. A non-linear regression analysis was conducted (GST-NΔ173 Tec (*black circles*), $n = 8$; SH1 kinase domain (*green squares*), $n = 5$; GST-PH-TH (*blue triangles*), $n = 3$; GST-SH3-SH2 (*red triangles*), $n = 3$; GST (*orange rhombuses*), $n = 5$), and S.E. values were calculated. As detailed under "Experimental Procedures," assuming a binding stoichiometry of 1:1, dissociation constants were calculated to be 1.434 ± 0.55 μM (S.E.) for GST-NΔ173 Tec and 1.032 ± 0.29 μM (S.E.) for the SH1 kinase domain of Tec. *B*, competition experiments for the interaction between SH1 kinase domain of Tec GST-NΔ173 Tec and fluorescein-labeled FGF2. Experiments were conducted as described above. Conditions in the absence and presence of unlabeled FGF2 (50 μM) were compared. All data points were normalized based on measurements on fluorescein-labeled FGF2 alone. Errors are given as S.E. An unpaired and one-tailed *t* test was conducted to assess statistical significance (*, $p < 0.05$; **, $p < 0.01$; ***, $p < 0.001$; ****, $p < 0.0001$). *C*, competition experiments for the interaction between GST-NΔ173 Tec and fluorescein-labeled FGF2. Experiments were conducted as described above. Conditions in the absence and presence of unlabeled FGF2 (50 μM) were compared. All data points were normalized based on measurements on fluorescein-labeled FGF2 alone. *Error bars*, S.E. An unpaired and one-tailed *t* test was conducted to assess statistical significance (*, $p < 0.05$; **, $p < 0.01$; ***, $p < 0.001$; ****, $p < 0.0001$).

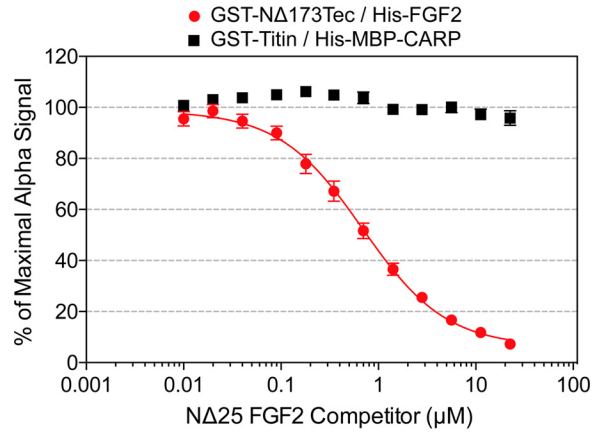

FIGURE 3. **A protein-protein interaction assay designed to screen small molecule libraries for compounds inhibiting FGF2 binding to Tec kinase.** The direct interaction between FGF2 and Tec kinase was quantified using Alpha® technology (*red spheres*). A His-tagged form of FGF2 (62.5 nM) and GST-NΔ173Tec (31.25 nM) were used along with glutathione-coated donor and Ni-NTA-coated acceptor beads as explained under "Experimental Procedures." As a specificity control, an unrelated protein pair, His-tagged MBP-CARP and GST-Titin (*black spheres*), was used. Alpha® signals were measured in the presence of increasing concentrations of untagged NΔ25FGF2, a competitor for binding of His-tagged FGF2 to GST-NΔ173 Tec. Alpha® signals are expressed as percentage of the median of the maximal Alpha® signal (tagged proteins in the absence of the NΔ25FGF2 competitor), which was set to 100% in each independent experiment. Data points represent the mean of eight independent experiments, each of which consisted of three technical replicates. Experimental deviations are expressed as S.E. (*error bars*). Data were fitted with a non-linear regression model. The K_D of the GST-NΔ173 Tec-N25ΔFGF2 complex was calculated to be 0.63 ± 0.033 μM (S.E.) ($r^2 = 0.9986$).

inhibitory potential of the identified compounds along with their inactive derivatives (Fig. 5). Using the Alpha® protein-protein interaction assay, IC_{50} values of 8.9 ± 1.1 μM (S.E.) for compound 6 (Fig. 5*A*), 7.0 ± 1.1 μM (S.E.) for compound 14 (Fig. 5*B*), and 11.7 ± 1.0 μM (S.E.) for compound 21 (Fig. 5*C*) were determined. By contrast, the inactive compounds 18 (Fig. 5*D*) and 19 (Fig. 5*E*) did not exert significant inhibition of the interaction between His-tagged FGF2 and GST-NΔ173 Tec at concentrations of up to 200 μM. Importantly, neither the active nor the inactive compounds affected the deselection assay probing for a potential inhibitory activity toward the unrelated interaction between Titin and CARP (Fig. 5, *A–E*). Also, none of the compounds were active in a technical control assay in which a single fusion protein (GST-His-Biotin) was used to directly link Alpha® donor and acceptor beads (Fig. 5, *A–E*). Our combined

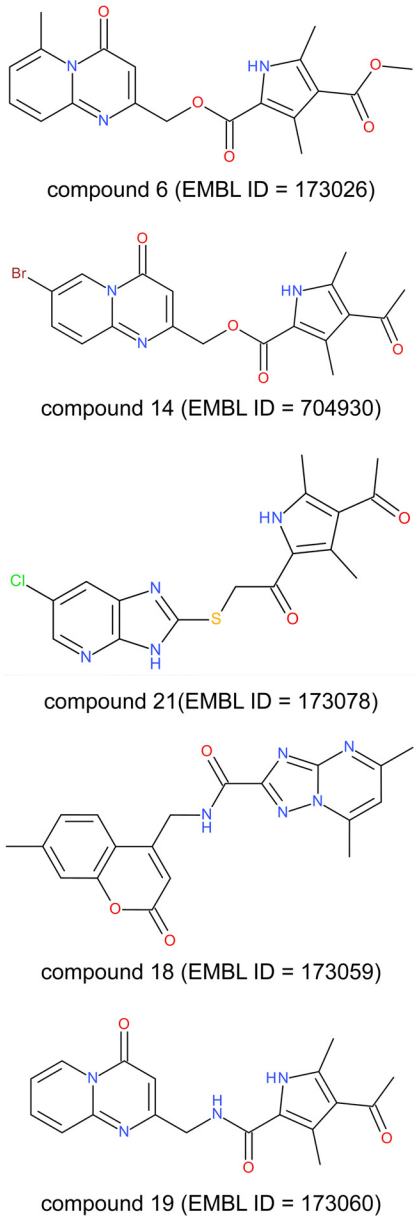

FIGURE 4. **Chemical structures of active (compounds 6, 14, and 21) and inactive (compounds 18 and 19) compounds.** EMBL IDs are provided as a reference to the internal database of the Chemical Biology Core Facility at EMBL Heidelberg (58).

findings from Fig. 5 establish compounds 6, 14, and 21 (Fig. 4) (58) as selective and potent inhibitors of the interaction between FGF2 and NΔ173 Tec that are characterized by IC50 values in the low micromolar range.

Small Molecule Inhibition of Tec Kinase-catalyzed Tyrosine Phosphorylation of FGF2—To analyze the potential of the active compounds beyond protein-protein interaction assays (Fig. 5), we tested whether they affect tyrosine phosphorylation of FGF2 mediated by Tec kinase (Fig. 6). Purified FGF2 and NΔ173 Tec were incubated under the conditions indicated. Tyrosine phosphorylation of both GST-NΔ173 Tec (autophosphorylation) and FGF2 was monitored by quantitative Western analysis using antibodies directed against a phosphopeptide derived from FGF2. These antibodies also recognized the autophosphorylated form of GST-NΔ173 Tec (Fig. 6*A*). Otherwise, they were found to be characterized by a low background recognition of non-phosphorylated FGF2 and Tec kinase (Figs. 6 and 7) and proved highly specific for the phosphorylated form of tyrosine 81 (Fig. 6, *D–F*), the key phosphorylation site targeted by Tec kinase (12, 24, 31). Protein amounts were monitored for all conditions employing SDS-PAGE and Coomassie staining (Fig. 6*B*). These experiments revealed potent inhibition of FGF2 tyrosine phosphorylation by the three active compounds 6, 14, and 21 (Fig. 6*A*). The Western analysis shown in Fig. 6*A* was quantified, revealing about 75% inhibition by compound 6 and almost quantitative inhibition by compounds 14 and 21 (Fig. 6*C*). Interestingly, autophosphorylation of NΔ173 Tec was affected as well, albeit less efficiently compared with FGF2 phosphorylation (Fig. 6, *A* and *C*). By contrast, the control compounds 18 and 19 affected neither NΔ173 Tec autophosphorylation nor FGF2 tyrosine phosphorylation (Fig. 6, *A* and *C*). Therefore, beyond the analysis of protein-protein interactions (Fig. 5), these experiments establish inhibitory potency of the identified active compounds with regard to FGF2 tyrosine phosphorylation mediated by Tec kinase.

Selectivity of Active Compounds Regarding Different Substrates of Tec Kinase—To test whether the active compounds 6, 14, and 21 selectively block Tec-mediated tyrosine phosphorylation of FGF2, we tested another established substrate of Tec, STAP1 (48, 49). In this independent set of experiments, the inhibitory potency of compounds 6, 14, and 21 toward Tec-mediated FGF2 tyrosine phosphorylation was confirmed (Fig. 7, *A* and *D*). Interestingly, the observed inhibition of Tec autophosphorylation was not only observed in the presence of FGF2 but, albeit less efficiently in case of compounds 6 and 21, in its absence as well (Fig. 7, *B* and *E*). This effect was particularly evident for compound 14. Finally, we tested whether the active compounds affect Tec-mediated tyrosine phosphorylation of STAP1 (Fig. 7, *C* and *F*). Intriguingly, in the presence of STAP1, neither autophosphorylation of NΔ173 Tec nor tyrosine phosphorylation of STAP1 was affected by any of the compounds we found active toward FGF2 phosphorylation. These findings suggest that the active compounds 6, 14, and 21 bind to Tec kinase and prevent recruitment of FGF2, resulting in a loss of FGF2 tyrosine phosphorylation. In the absence of a bound substrate, autophosphorylation of NΔ173 Tec is inhibited as well. However, in the presence of an unrelated substrate, such as STAP1, neither autophosphorylation of NΔ173 Tec nor tyrosine phosphorylation of STAP1 is affected by any of the compounds 6, 14, and 21. Therefore, our combined findings establish selectivity of these inhibitors toward FGF2 as a substrate of Tec, reflecting the design of the original small molecule screening procedure aiming at FGF2/Tec protein-protein interaction inhibitors.

Active Compounds Targeting the Interaction between Tec Kinase and FGF2 Inhibit Tyrosine Phosphorylation of FGF2 in Cells—A first set of experiments in cells was conducted to analyze whether the active compounds 6, 14, and 21 inhibit tyrosine phosphorylation of FGF2 in cells (Fig. 8). Briefly, cells were induced with doxycycline to express FGF2-GFP in the presence of active (compounds 6, 14, and 21) and inactive (compounds 18 and 19) compounds as well as under mock conditions (for details, see "Experimental Procedures"). FGF2-GFP fusion proteins were affinity-purified under the conditions indicated

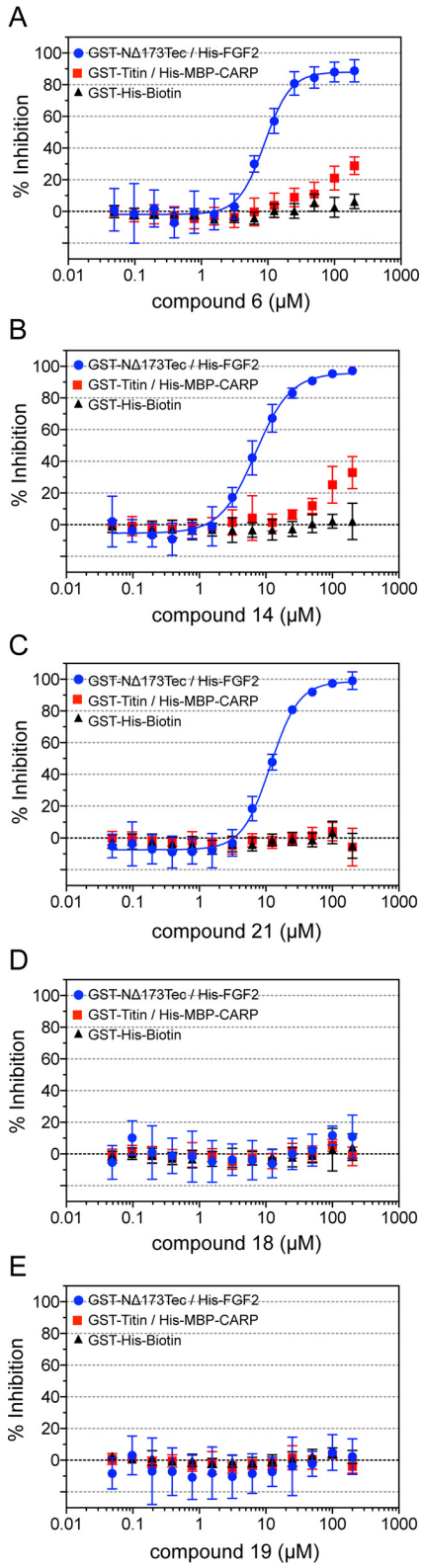

FIGURE 5. **Determination of dose-response curves for active (compounds 6, 14, and 21) *versus* inactive (compounds 18 and 19) compounds.** Alpha® protein-protein interaction assays with His-tagged FGF2 (125 nM) and GST-NΔ173 Tec (30 nM) (*blue spheres*) as well as His-tagged MBP-CARP (20 nM) and GST-titin (20 nM) (*red squares*) were conducted as described in the legend to Fig. 3 and under "Experimental Procedures." Additionally, as a technical control, a single fusion protein containing both a GST and a His tag was used (20 nM; *black triangles*). Dose-response curves were recorded with the three active compounds (compounds 6, 14, and 21) as well as the two control compounds (compounds 18 and 19) shown in Fig. 4 (58). For each compound, four independent experiments (each of which was conducted in three technical replicates) were performed. Data points were fitted using the non-linear regression function log (inhibitor) *versus* response − variable slope (four parameters). Data were evaluated using GraphPad Prism (version 5 for Macintosh OS X). *Error bars*, S.D. *A*, dose-response curves of compound 6. IC_{50} (His-FGF2/GST-NΔ173 Tec) = 8.9 ± 1.1 μM (S.E.). *B*, dose-response curves of compound 14. IC_{50} (His-FGF2/GST-NΔ173 Tec) = 7.0 ± 1.1 μM (S.E.). *C*, dose-response curves of compound 21. IC_{50} (His-FGF2/GST-NΔ173 Tec) = 11.7 ± 1.0 μM (S.E.). *D*, dose-response curves of compound 18. *E*, dose-response curves of compound 19.

using GFP trap magnetic beads and analyzed by quantitative Western blotting (Fig. 8*A*). Total FGF2-GFP was quantified with an affinity-purified anti-FGF2 antibody (26, 50). Tyrosine phosphorylation of FGF2-GFP was monitored using the anti-Tyr(P) antibody 4G10 (Merck Millipore). The LI-COR dual channel imaging platform was used to quantify tyrosine-phosphorylated FGF2-GFP normalized by the amount of total FGF2-GFP (Fig. 8*B*). These experiments revealed that all three active compounds inhibit tyrosine phosphorylation of FGF2 in cells. By contrast, compared with mock conditions, the inactive control compounds 18 and 19 did not inhibit this process to a significant extent. Intriguingly, although the active compounds 14 and 21 showed partial inhibition, the most active inhibitor was compound 6 that blocked tyrosine phosphorylation of FGF2 down to background levels (Fig. 8*B*). These experiments demonstrate that, beyond the *in vitro* reconstitution experiments shown in Figs. 5–7, the identified Tec/FGF2 protein-protein interaction inhibitors are capable of inhibiting tyrosine phosphorylation of FGF2 in a cellular context.

Small Molecule Inhibitors Blocking FGF2 Tyrosine Phosphorylation Inhibit FGF2 Secretion from Cells—Based upon the biochemical reconstitution experiments shown in Figs. 5–7 and the cell-based experiments shown in Fig. 8, we investigated whether the active compounds 6, 14, and 21 influence FGF2 secretion from cells (Fig. 9). Again, the inactive compounds 18 and 19 were taken as negative controls. To quantify FGF2 secretion, a well established biotinylation assay was used to detect FGF2 bound to heparan sulfates on cell surfaces (23, 26, 51). Briefly, following doxycycline-induced expression of FGF2-GFP, proteins present on cell surfaces were modified using a membrane-impermeable biotinylation reagent. Following cell lysis, biotinylated proteins (cell surface) were separated from non-biotinylated proteins (intracellular) using streptavidin beads. Samples were subjected to SDS-PAGE followed by a Western analysis of FGF2-GFP and GAPDH, the latter being a control for a protein restricted to the intracellular environment. Cell surface biotinylation of FGF2-GFP was analyzed under various experimental conditions, comparing a mock control with a titration (10, 25, and 50 μM) of both active (compounds 6, 14, and 21) and inactive (compounds 18 and 19) compounds (Fig. 9). Under these conditions, cell surface signals for FGF2-GFP were quantified using the LI-COR imaging platform. This analysis revealed all active compounds identified in the experiments shown in Figs. 5–8 to significantly inhibit FGF2 secretion from cells (Figs. 8 (*B* and *C*) and 9*A*). Importantly, the most active inhibitor (compound 6) identified in the cell-based experiments shown in Fig. 8 was also the most efficient one with regard to inhibition of FGF2 secretion. For com-

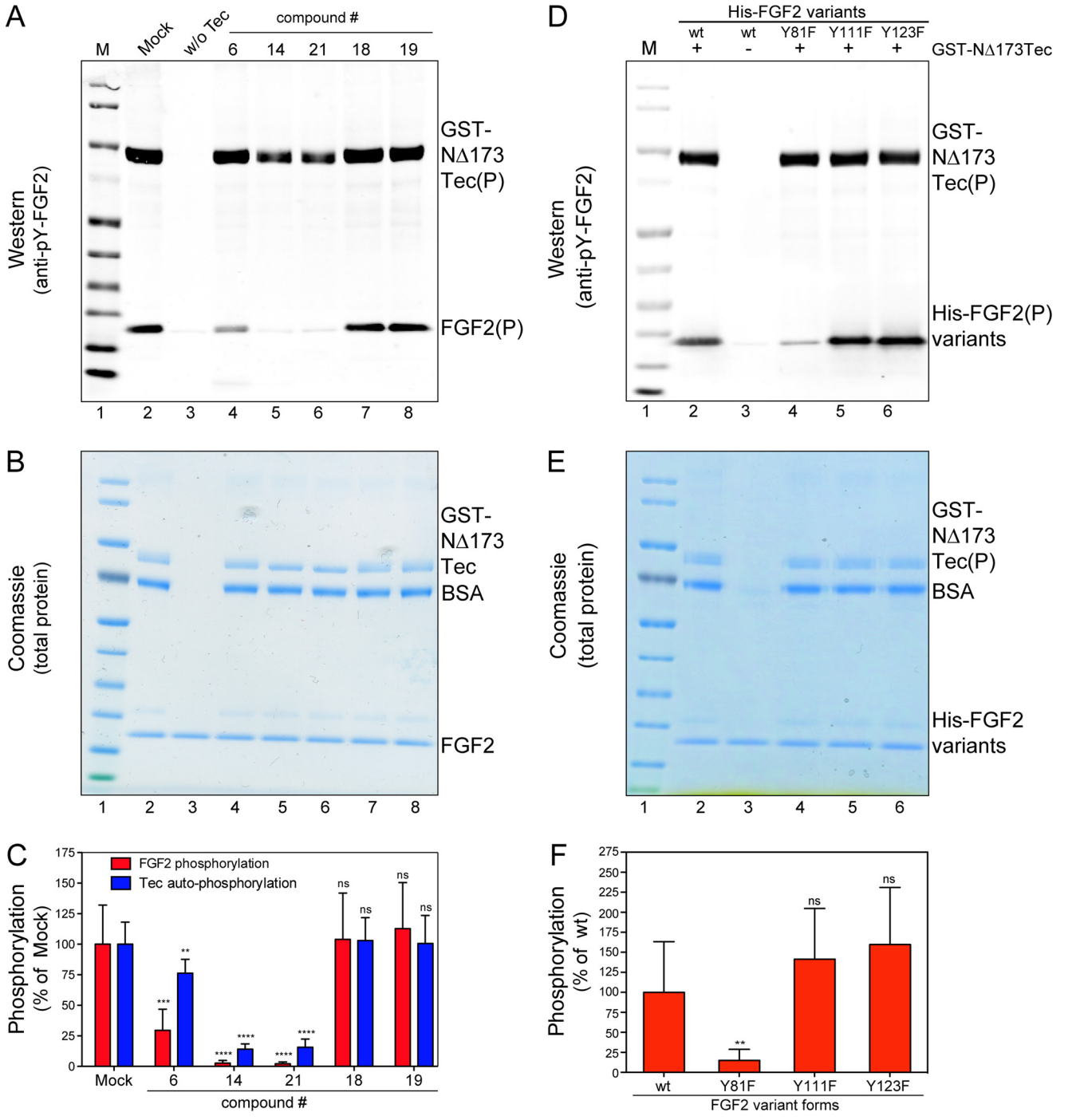

FIGURE 6. **Small molecule inhibition of Tec kinase-mediated tyrosine phosphorylation of FGF2.** FGF2 tyrosine phosphorylation and Tec kinase autophosphorylation were reconstituted with purified components based on Western analysis using anti-phosphotyrosine antibodies directed against an FGF2-derived phosphopeptide. *In vitro* phosphorylation experiments were conducted in the absence (1% DMSO mock control) and presence of the small molecule inhibitors (compounds 6, 14, and 21; 50 μM in 1% DMSO) and control compounds (compounds 18 and 19; 50 μM in 1% DMSO) introduced in Figs. 4 (58) and 5. Fluorescent secondary antibodies were used to detect antigens, employing the LI-COR Odyssey imaging platform. *M*, PageRuler prestained protein ladder (140, 115, 80, 65, 50, 40, 30, 25, 15, and 10 kDa). For details, see "Experimental Procedures." *A*, representative Western analysis using antibodies recognizing both phosphorylated FGF2 (*FGF2(P)*) and Tec kinase in its autophosphorylated form (*GST-NΔ173 Tec(P)*). *B*, Coomassie-stained SDS gel corresponding to the Western analysis shown in *A*. *C*, quantification and statistical analysis of five independent experiments (corresponding to the example shown in *A* and *B*) using the LI-COR Odyssey imaging platform. Following background normalization, the average of FGF2 tyrosine phosphorylation under mock conditions was defined as 100% activity. *Error bars*, S.D. A one-tailed and unpaired *t* test was conducted to test significance (*, $p < 0.05$; **, $p < 0.01$; ***, $p < 0.001$; ****, $p < 0.0001$). *NS*, absence of significant differences. *D*, representative Western analysis using His-tagged variant forms of FGF2 (WT, Y81F, Y111F, and Y123F, as indicated) to characterize the anti-phosphotyrosine-FGF2 antibody used in *A*. *E*, Coomassie-stained SDS gel corresponding to the Western analysis shown in *D*. *F*, quantification and statistical analysis of six independent experiments (corresponding to the example shown in *D* and *E*) using the LI-COR Odyssey imaging platform. Following background normalization, the average of tyrosine phosphorylation of FGF2 wild-type was defined as 100% activity. S.D. values are shown. A one-tailed and unpaired *t* test was conducted to test significance (*, $p < 0.05$; **, $p < 0.01$; ***, $p < 0.001$; ****, $p < 0.0001$). *NS*, absence of significant differences.

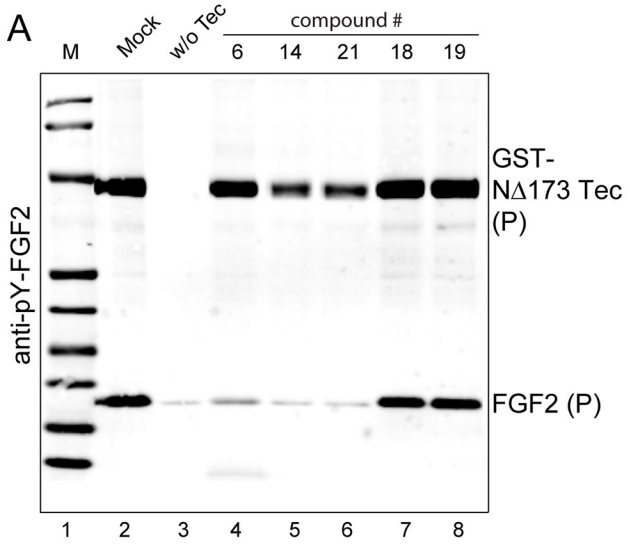
A
M
Mock
w/o Tec
compound #
6
14
21
18
19
anti-pY-FGF2
GST-
NΔ173 Tec
(P)
FGF2 (P)
1
2
3
4
5
6
7
8

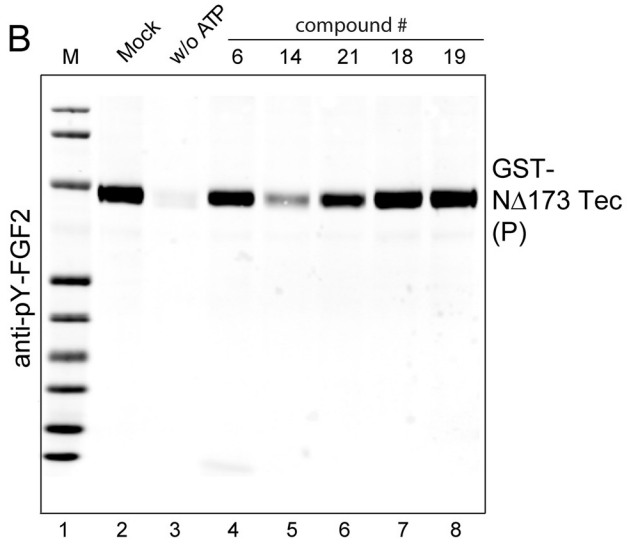
B
M
Mock
w/o ATP
compound #
6
14
21
18
19
anti-pY-FGF2
GST-
NΔ173 Tec
(P)
1
2
3
4
5
6
7
8

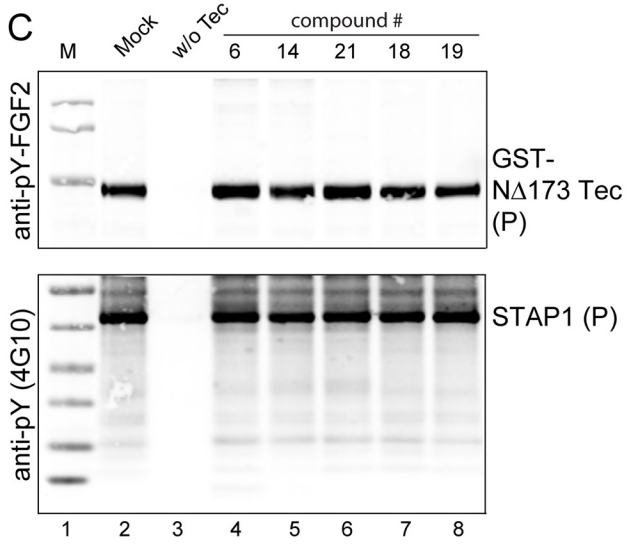
C
M
Mock
w/o Tec
compound #
6
14
21
18
19
anti-pY-FGF2
GST-
NΔ173 Tec
(P)
anti-pY (4G10)
STAP1 (P)
1
2
3
4
5
6
7
8

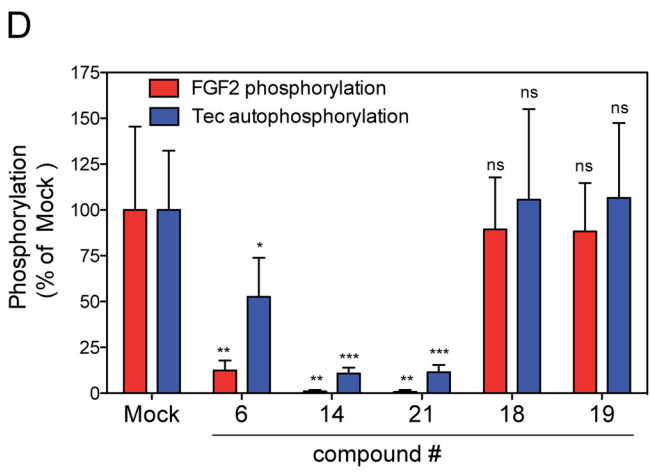
D
FGF2 phosphorylation
Tec autophosphorylation
Phosphorylation
(% of Mock)
175
150
125
100
75
50
25
0
ns
*
**
***
Mock
6
14
21
18
19
compound #

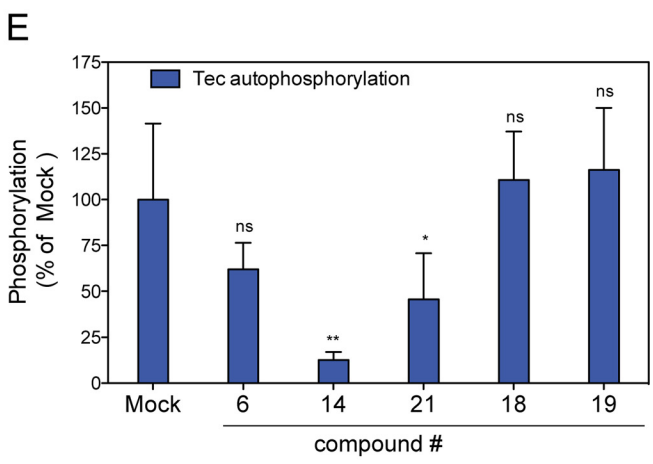
E
Tec autophosphorylation
Phosphorylation
(% of Mock)
175
150
125
100
75
50
25
0
ns
*
**
Mock
6
14
21
18
19
compound #

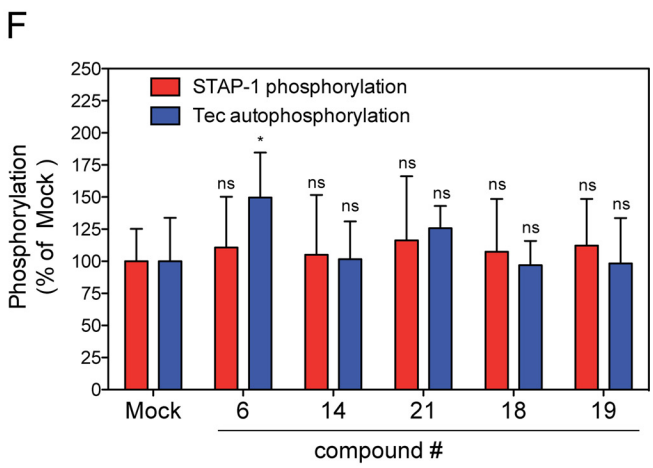
F
STAP-1 phosphorylation
Tec autophosphorylation
Phosphorylation
(% of Mock)
250
225
200
175
150
125
100
75
50
25
0
ns
*
Mock
6
14
21
18
19
compound #

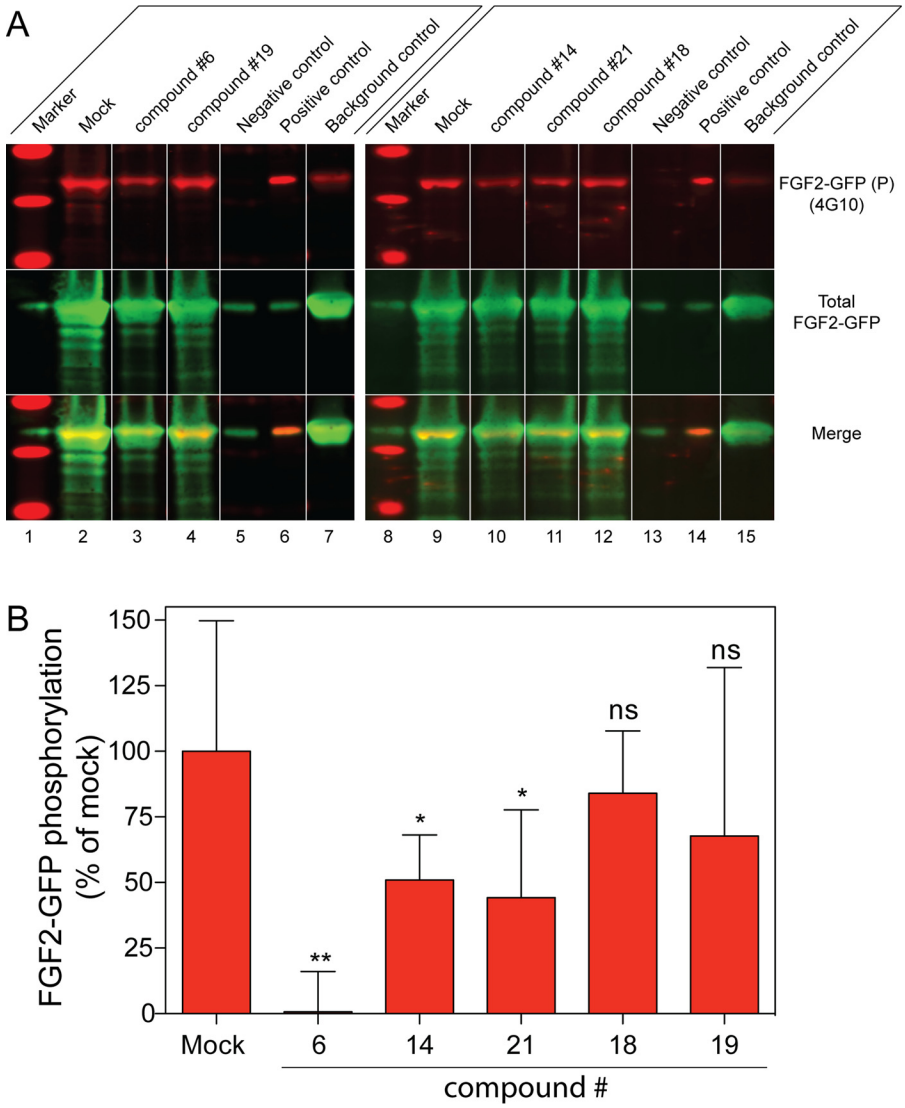

FIGURE 8. **Small molecule protein-protein interaction inhibitors of the Tec-FGF2 complex block tyrosine phosphorylation of FGF2 in cells.** CHO cells were induced with doxycycline to express FGF2-GFP fusion proteins under the conditions indicated (see "Experimental Procedures" for details). All compounds were used at a final concentration of 50 μM in 0.5% DMSO. The mock controls correspond to 0.5% DMSO in the absence of compound. Following cell lysis, FGF2-GFP fusion proteins were affinity-purified employing GFP trap magnetic beads. Proteins were eluted with SDS sample buffer and subjected to SDS-PAGE. Following Western blotting, the LI-COR imaging platform was used to quantify both tyrosine phosphorylation (4G10) and total FGF2-GFP (anti-FGF2). In addition to samples derived from cells (*lanes 2–4* and *9–12*), recombinant FGF2-GFP (2 ng) and *in vitro* phosphorylated FGF2-GFP (2 ng) were used as negative and positive controls for FGF2 tyrosine phosphorylation (*lanes 5* and *6* and *lanes 13* and *14*). 165 ng of recombinant FGF2-GFP (an amount comparable with the material isolated from cells) were used to quantify the background of the 4G10 anti-phosphotyrosine antibody (*lanes 7* and *15*). In *lanes 1* and *8*, marker proteins of 50, 40, and 30 kDa are shown. *A*, quantitative Western analysis of affinity-purified FGF2-GFP fusion proteins from cells cultivated under the conditions indicated. *B*, quantification and statistical evaluation of the Western analysis shown in *A*. FGF2 phosphotyrosine signals (4G10) were normalized by total FGF2-GFP. The statistical analysis was based upon four independent biological replicates. *Error bars,* S.D. A one-tailed and unpaired *t* test was conducted to reveal significant differences between the mock control and conditions in the presence of compounds (*, $p < 0.05$; **, $p < 0.01$). *ns*, absence of significant differences.

FIGURE 7. **Selectivity of small molecule inhibitors toward Tec kinase-mediated tyrosine phosphorylation of FGF2.** FGF2 and STAP1 tyrosine phosphorylation as well as Tec kinase autophosphorylation were analyzed as described in the legend to Fig. 6 and under "Experimental Procedures." *In vitro* phosphorylation experiments were conducted in the absence (1% DMSO mock control) and presence of the small molecule inhibitors (compounds 6, 14, and 21; 50 μM in 1% DMSO) and control compounds (compounds 18 and 19; 50 μM in 1% DMSO) introduced in Figs. 4 (58) and 5. Western analysis was conducted using anti-phosphotyrosine antibodies (anti-Tyr(P)-FGF2 for FGF2 and Tec as well as anti-Tyr(P)-4G10 for STAP1). *M*, PageRuler prestained protein ladder: 140, 115, 80, 65, 50, 40, 30, 25, 15, and 10 kDa. Fluorescent secondary antibodies were used to detect and quantify antigens using the LI-COR Odyssey imaging platform. In *D–F*, following normalization based upon background signals detected in the absence of Tec kinase or ATP, the average of the signals detected under mock conditions was defined as 100% activity. *Error bars*, S.D. A one-tailed and unpaired *t* test was conducted to assess statistical significance (*, $p < 0.05$; **, $p < 0.01$; ***, $p < 0.001$; ****, $p < 0.0001$). *ns*, absence of significant differences. *A*, Tec kinase-mediated tyrosine phosphorylation of FGF2 in the absence and presence of active and inactive compounds (50 μM each). *B*, Tec autophosphorylation in the absence of a substrate measured in the absence and presence of active and inactive compounds (50 μM each). *C*, Tec kinase-mediated tyrosine phosphorylation of STAP1 in the absence and presence of active and inactive compounds (50 μM each). Following protein transfer to PVDF, membranes were cut to stain the upper part with anti-Tyr(P)-FGF2 antibodies (to detect Tec autophosphorylation) and the lower part with anti-Tyr(P)-4G10 antibodies (to detect phosphorylated STAP1). *D*, quantification of the Western analysis shown in *A*. *E*, quantification of the Western analysis shown in *B*. *F*, quantification of the Western analysis shown in *C*.

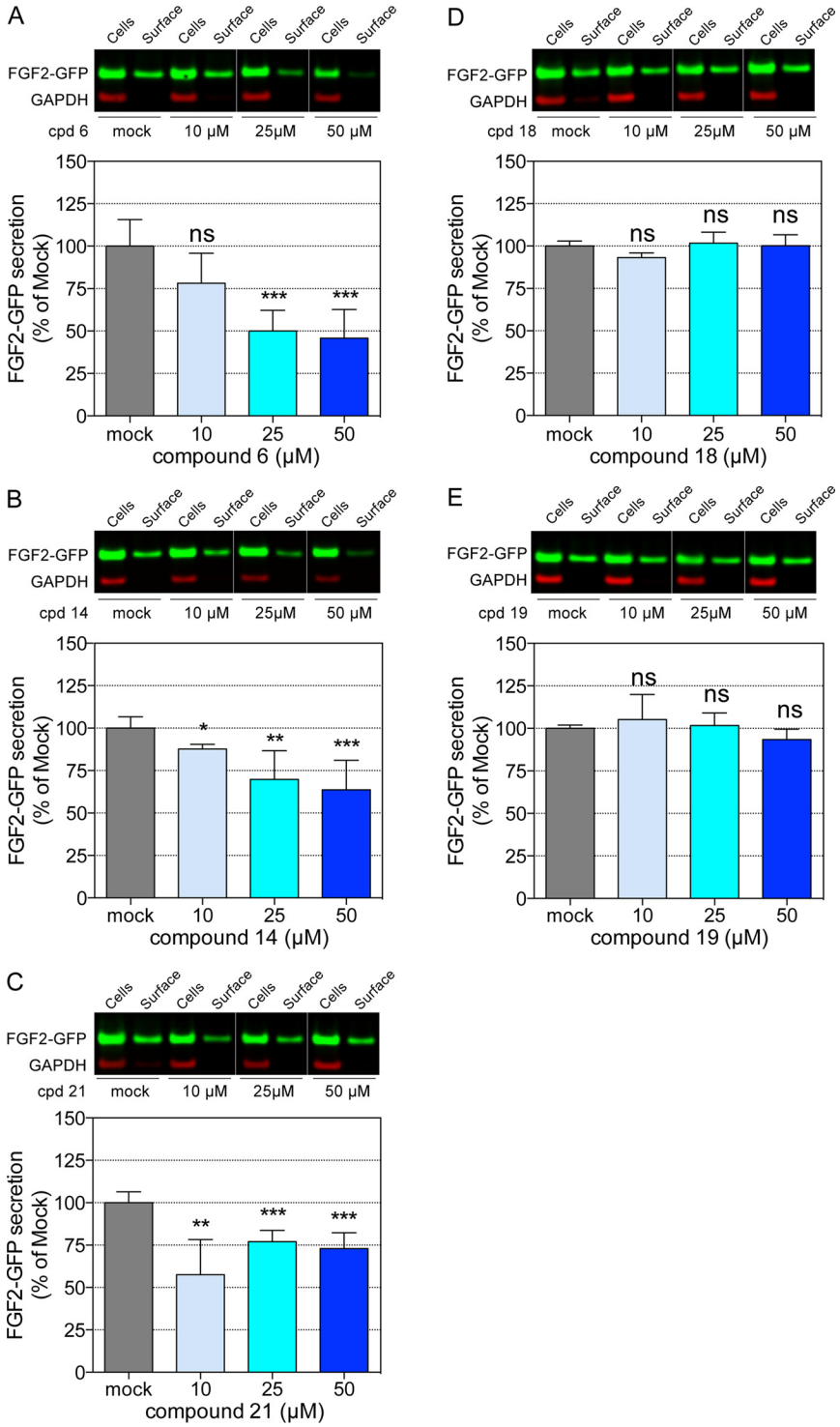

FIGURE 9. **Small molecule inhibitors blocking Tec kinase mediated tyrosine phosphorylation of FGF2 inhibit unconventional secretion of FGF2 from cells.** A stable CHO cell line expressing a FGF2-GFP fusion protein in a doxycycline-dependent manner was used to quantify FGF2 transport to cell surfaces in the absence and presence of the small molecule inhibitors introduced in Figs. 4–7 (58). As detailed under "Experimental Procedures," following cultivation of cells in the presence of compounds as indicated and induction of FGF2-GFP expression, proteins localized to the cell surface were biotinylated with a membrane-impermeable reagent. Following quenching of the biotinylation reagent, biotinylated proteins were purified using streptavidin beads. Following SDS-PAGE analyzing both the total lysate (input termed *Cells*; 1.7%) and the biotinylated cell surface fraction (33%), a Western analysis was conducted to detect the secreted population of FGF2-GFP. Using appropriate fluorescent secondary antibodies, both FGF2-GFP and GAPDH (used as a control protein restricted to the intracellular space) were quantified using the LI-COR Odyssey imaging platform. FGF2-GFP secretion quantified under mock conditions (0.5% DMSO) was defined as 100% secretion efficiency. *Error bars*, S.D. values from three independent experiments, each of which was conducted in two technical replicates. A two-tailed and unpaired *t* test was conducted to assess statistical significance (*, $p < 0.05$; **, $p < 0.01$; ***, $p < 0.001$; ****, $p < 0.0001$). *ns*, absence of significant differences. *A*, quantification of FGF2-GFP secretion from cells in the absence and presence of compound 6 (active). *B*, quantification of FGF2-GFP secretion from cells in the absence and presence of compound 14 (active). *C*, quantification of FGF2-GFP secretion from cells in the absence and presence of compound 21 (active). *D*, quantification of FGF2-GFP secretion from cells in the absence and presence of compound 18 (inactive). *E*, quantification of FGF2-GFP secretion from cells in the absence and presence of compound 19 (inactive).

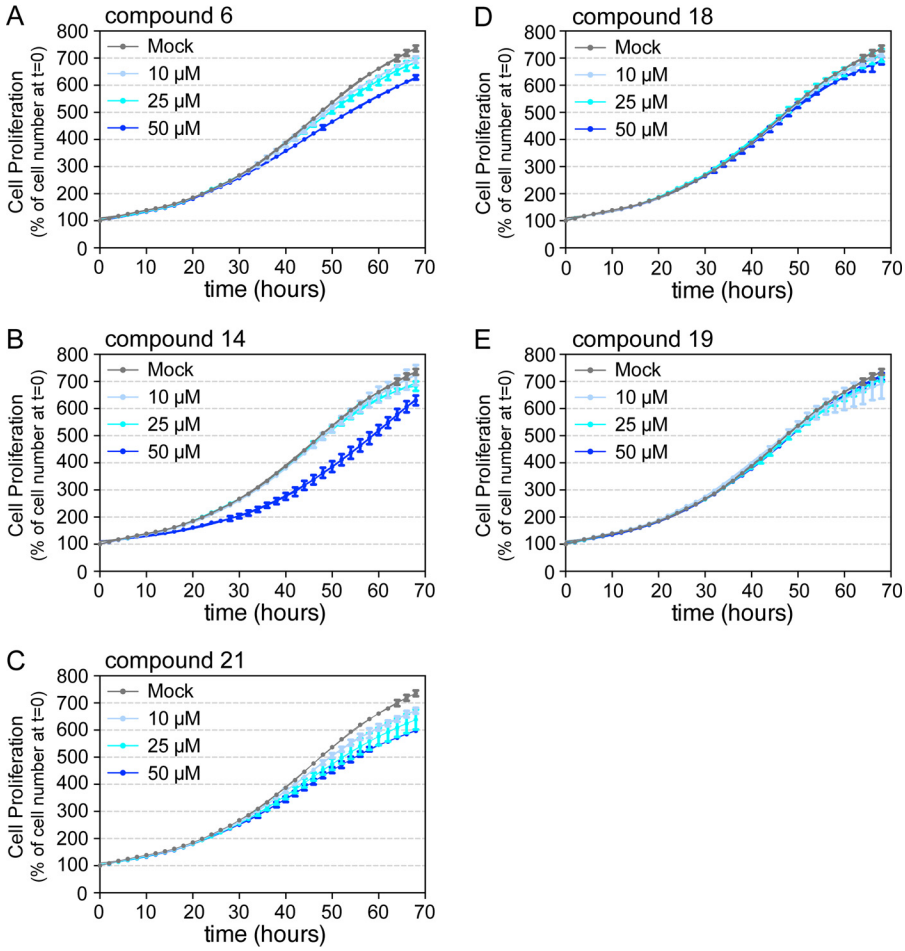

FIGURE 10. **Small molecule inhibitors blocking Tec kinase-mediated tyrosine phosphorylation of FGF2 do not exert apparent pleiotropic effects on cell viability and proliferation.** CHO cells expressing mCherry fused to a nuclear localization signal were used to monitor potential pleiotropic effects on cell viability and proliferation of the compounds introduced in Fig. 4 (58). Cell proliferation was monitored by absolute counting of fluorescent nuclei using an IncuCyte Zoom live cell imaging microscope (Essen Biosciences). As a starting density, 1×10^4 cells were cultivated per experimental condition in 96-well plates. The actual cell number measured at $t = 0$ was set to 100%. Cell proliferation was monitored at 37 °C for 72 h under mock conditions (0.5% DMSO) as well as in the presence of 10, 25, and 50 μM concentrations of compounds 6 (*A*), 14 (*B*), 21 (*C*), 18 (*D*) and 19 (*E*). Cell numbers were determined in intervals of 2 h. The experiments shown are representative of a total of four biological replicates, each of which contained three technical replicates for every single data point. *Error bars*, S.D.

pounds 6 and 14, inhibition was observed in a dose-dependent manner. In the case of the active compound 21, inhibition was stronger at 10 μM compared with higher concentrations. This observation might be related to solubility issues because aggregates of compound 21 were increasingly observable at concentrations of 25 and 50 μM (data not shown). Importantly, the inactive compounds 18 and 19 did not affect FGF2 secretion from cells (Fig. 9, *D* and *E*). In addition, neither the active nor the inactive compounds exerted substantial pleiotropic effects on cell proliferation (Fig. 10). Using an IncuCyte Zoom live cell imaging platform, we quantified cell proliferation under mock conditions *versus* the presence of active and inactive compounds. Although a modest decrease of cell proliferation could be observed, cells were viable and continued to proliferate under all experimental conditions (Fig. 10). Our combined findings establish the active compounds 6, 14, and 21 as potent and selective inhibitors of Tec kinase-mediated tyrosine phosphorylation (Figs. 5–8) that are also functional in a cellular context inhibiting FGF2 secretion (Figs. 9 and 10).

Discussion

The unconventional mechanism by which FGF2 is secreted from tumor cells has been worked out in considerable detail (12). FGF2 exits cells by direct translocation across the plasma membrane (18, 19). This process involves (i) membrane recruitment at the inner leaflet mediated by the phosphoinositide $PI(4,5)P_2$ (1, 2, 21, 22), (ii) FGF2 oligomerization and membrane pore formation (9, 11, 23, 24, 30), and (iii) extracellular trapping mediated by membrane-proximal heparan sulfate proteoglycans (25, 26). In addition, Tec kinase (9, 31) and ATP1A1 (12, 32–34), two additional factors physically associated with the plasma membrane, have been shown to play critical roles in the unconventional secretory pathway of FGF2 (12). Whereas ATP1A1 is an integral membrane protein, Tec kinase contains a PH domain and associates with the inner leaflet via recruitment by the phosphoinositide $PI(3,4,5)P_3$ (36, 37). The precise role of ATP1A1 in unconventional secretion of FGF2 is unknown (12). By contrast, Tec kinase was shown to directly interact

with and phosphorylate FGF2, an activity causing increased membrane pore formation by FGF2 oligomers (11, 12, 24, 31).

In the current study, based upon the stimulatory function of Tec kinase in unconventional secretion of FGF2, we aimed at the identification of small molecule inhibitors that prevent Tec kinase from binding to FGF2. In turn, we hypothesized that such compounds would cause a failure of efficient tyrosine phosphorylation of FGF2 along with inhibition of FGF2 secretion from cells. Following a characterization of the interaction between FGF2 and Tec kinase identifying the SH1 kinase domain of Tec as the FGF2 binding site with submicromolar affinity, a scaffold-based library of 79,000 small molecules was screened for protein-protein interaction inhibitors using Alpha® technology (47). Following primary screening, hits were reevaluated by determining dose-response curves focusing on compounds with IC_{50} values <100 μM. Beyond the protein-protein interaction assays, inhibitors were further characterized by their potential to block Tec kinase-mediated tyrosine phosphorylation of FGF2. The combination of these secondary assays revealed three active compounds characterized by IC_{50} values in the low micromolar range (7, 9, and 12 μM, respectively) along with two structurally related compounds that were found inactive under all conditions. Beyond inhibition of FGF2 tyrosine phosphorylation, the active compounds also inhibited Tec kinase autophosphorylation. This effect was observed both in the presence and absence of FGF2. Therefore, our combined findings suggest that the identified molecules bind to Tec kinase, inhibit autophosphorylation, and prevent recruitment of FGF2 as a substrate of Tec kinase. Intriguingly, tyrosine phosphorylation of a different substrate, STAP1 (48, 49), was unaffected in the presence of the active compounds. Moreover, Tec autophosphorylation was also at normal levels under these conditions. Although the structural basis for these differences is currently unknown, these findings demonstrate the potential of the identified small molecules as selective inhibitors of Tec kinase-mediated tyrosine phosphorylation of FGF2.

Beyond the biochemical reconstitution experiments, we also demonstrated the ability of the active compounds to inhibit tyrosine phosphorylation of FGF2 in cells. In turn, correlated with their differential inhibitory potentials, these compounds also interfered with FGF2 secretion from cells. Although inhibition of FGF2 transport to the cell surface was not complete, all three active compounds exerted inhibition of FGF2 secretion of up to 50% in a statistically significant manner. Whereas compounds 6 and 14 did so in a dose-dependent manner, compound 21 showed robust inhibition at 10 μM and somewhat less efficient inhibition at 25 and 50 μM, respectively. The latter observation may be due to solubility issues that were observed for compound 21 at higher concentrations in the context of cell culture medium. In contrast to compounds 6, 14, and 21, the structurally related but inactive control compounds (compounds 18 and 19) did not affect FGF2 secretion from cells. None of the compounds affected general cell viability as measured by proliferation efficiencies. These findings suggest that, in a cellular context, the family of structurally related compounds described in this study does not cause pleiotropic effects to a significant extent.

Although the limited number of active compounds described in this study is insufficient to establish a full structure-activity relationship, there is clear guidance on how to proceed in subsequent chemical synthesis. These preliminary findings include the following: (i) substitutions at the pyrrole moiety are tolerated, (ii) replacement of ester linkages is tolerated under some circumstances, and (iii) rescaffolding of the pyrido-pyrimidone scaffold is possible. Based on these modifications, defined pairs of compounds will be synthesized in future studies, a strategy that will allow for a clean determination of the structure-activity relationship of the new class of Tec kinase inhibitors described in this work. These efforts will also aim at derivatives characterized by improved IC_{50} values along with systematic improvement of the balance between water solubility and membrane permeability to target the Tec-FGF2 complex inside cells.

In conclusion, we report the structures of the first inhibitors that have been specifically developed to block an unconventional secretory mechanism. Our findings establish the identified small molecules as useful lead compounds for the development of further Tec kinase inhibitors with drug-like properties. Such drugs carry great potential to prevent the action of FGF2 as a tumor cell survival factor, with small cell lung cancers being a prominent example (45, 46). However, such inhibitors might have an even broader impact because cancer cells are characterized by strong overexpression of PI3Ks, the enzymes synthesizing $PI(3,4,5)P_3$. Because Tec kinases are recruited to the inner leaflet via $PI(3,4,5)P_3$ (52) and FGF2 is highly overexpressed in many tumors (41, 43, 44), drugs preventing Tec-mediated tyrosine phosphorylation of FGF2 carry great potential for cancer therapy. Beyond their biomedical implications as lead compounds for drug development, the identified small molecule inhibitors corroborate the role of Tec kinase as a stimulatory component of the unconventional secretory pathway of FGF2. They further represent useful tool compounds to study the mechanism of unconventional secretory processes in general, in particular with regard to other cargoes, such as HIV-Tat (27–30).

Experimental Procedures

Expression and Purification of Recombinant Proteins—Several recombinant forms of both FGF2 and Tec kinase were used in this study. These included authentic FGF2 (154 amino acids; 18-kDa form), His-tagged FGF2 (including the variant forms Y81F, Y111F, and Y123F), and NΔ25FGF2 (129 amino acids) as well as four forms of Tec kinase with the domain structures depicted in Fig. 1*A* (GST-NΔ173 Tec, GST-PH-TH, GST-SH3-SH2, and the SH1 kinase domain).

All forms of FGF2 were expressed and purified from *E. coli* according to standard procedures (23, 24). Untagged FGF2 was expressed as an N-terminal GST fusion protein. Following binding to glutathione affinity beads (glutathione-Sepharose™ 4 Fast Flow, GE Healthcare), the GST tag was cleaved off by thrombin treatment. The product was collected and loaded onto a heparin affinity column (HiTrap Heparin HP, GE Healthcare), and, following elution under high salt conditions, a homogeneous fraction of untagged FGF2 was collected. His-tagged FGF2 was purified by Ni-NTA affinity (HisTrap FF, GE

Healthcare) and heparin affinity chromatography. N-terminally truncated FGF2 (NΔ25FGF2; 129 amino acids) lacking the first 25 amino acids was expressed and purified to homogeneity using heparin affinity chromatography. Purified His-STAP1 was purchased from Hölzel Diagnostika (catalog no. GWB-P0486E-100).

All Tec kinase-derived constructs depicted in Fig. 1*A* (GST-NΔ173 Tec, GST-PH-TH, GST-SH3-SH2, and the SH1 kinase domain) were expressed in SF9 insect cells using the baculovirus expression system (53). GST-NΔ173 Tec, GST-PH-TH, and GST-SH3-SH2 were purified by glutathione affinity chromatography (GSTrap™ FF, GE Healthcare). By contrast, the SH1 kinase domain was purified based on an N-terminal His tag employing Ni-NTA affinity chromatography. The His tag was removed proteolytically followed by a second purification step based on size exclusion chromatography (HiLoad 16/600 Superdex™ 200 pg, GE Healthcare), yielding a homogeneous preparation of the SH1 kinase domain.

Pull-down Experiments Using FGF2-conjugated Epoxy Beads and Various Forms of Tec Kinase (Fig. 1)—FGF2 (2 mg; untagged 18-kDa form) was covalently conjugated to epoxy-activated Sepharose™ beads 6B (600 mg; catalog no. 17-0480-01, GE Healthcare) based on the manufacturer's instructions. FGF2-conjugated beads (final concentration = 0.2 μM FGF2) was incubated on a rotating platform for 2 h at room temperature with each of the Tec variant forms depicted in Fig. 1*A* (final concentration = 1.5 μM in a total volume of 200 μl). The binding buffer contained 50 mM Tris-HCl (pH 7.4), 150 mM NaCl, 1 mM benzamidine, 0.05% Tween 20, 1 mM DTT. Proteins bound to beads were collected by centrifugation (7000 × *g*, 4 °C, 5 min). The beads were washed extensively with binding buffer. Bound proteins were eluted with SDS sample buffer, and, following boiling at 95 °C, bound (100%) and unbound (1%) fractions were analyzed by SDS-PAGE (Novex NuPAGE 4–12% BisTris/MOPS precast gels). Protein gels were stained with Coomassie InstantBlue (Expedeon). Marker proteins of 140, 115, 80, 65, 50, 40, 30, 25, 15, and 10 kDa (PageRuler prestained protein ladder; catalog no. 26616, Thermo Scientific) were used to monitor migration behavior of proteins.

Determining the Dissociation Constant for the Interaction between Tec Kinase and FGF2 Employing Steady-state Fluorescence Polarization (Fig. 2)—To determine binding affinity between Tec kinase and FGF2, steady-state fluorescence polarization was used (54). His-tagged FGF2 was labeled with fluorescein-5-maleimide (F150, Thermo Fisher Scientific) covalently modifying a cysteine residue on the molecular surface of FGF2. Briefly, 100 nmol of His-tagged FGF2 (dissolved in 50 mM Tris-HCl, 150 mM NaCl, pH 7.4) were incubated with a 10-fold molar excess of tris(2-carboxyethyl)phosphine hydrochloride (Pierce) at room temperature. Fluorescein-5-maleimide (44 nmol) was added, resulting in a final volume of 0.8 ml. Following incubation for 20 min at room temperature, residual amounts of free dye were removed using PD-10 desalting columns (GE Healthcare). The labeled protein was concentrated using a Vivaspin 500 system with a cut-off of 10 kDa (Sartorius). Based on the manufacturer's instructions (F150, Thermo Fisher Scientific) using the extinction coefficient of fluoroscein 5-maleimide and the absolute protein concentration, the degree of labeling of His-tagged FGF2 was determined to be 30%. The final preparation of fluorescein-labeled FGF2 had a protein concentration of 1.7 mg/ml. All proteins used in these assays were adjusted to the same buffer (50 mM Tris-HCl, 150 mM NaCl, pH 7.4) using PD-10 desalting columns (GE Healthcare). Absolute protein concentrations were determined based upon the extinction coefficients and the molecular weights of each protein measuring absorption at 280 nm using a NanoDrop 1000 spectrophotometer.

To determine the dissociation constants for the interaction of FGF2 with various forms of Tec kinase, fluorescein-labeled FGF2 (50 nM) was incubated with increasing concentrations (0–20 μM, as indicated) of GST-NΔ173 Tec, GST-PH-TH, GST-SH3-SH2, and the SH1 kinase domain of Tec (Fig. 2*A*). In addition, GST alone was taken as a negative control. Following incubation for 3 h at room temperature in binding buffer (50 mM Tris-HCl, 150 mM NaCl, pH 7.4, 0.1% BSA, 0.05% Tween 20; final volume = 10 μl), steady-state fluorescence polarization experiments were conducted by excitation of labeled FGF2 with polarized light at a wave length of 492 nm. The interaction between fluorescein-labeled FGF2 and unlabeled forms of Tec kinase was measured at 515 nm as the progressive increase of fluorescence polarization (ΔPolarization) as a function of the protein concentration of the various forms of Tec kinase. Samples were measured in black low volume 384-well plates (catalog no. 6008260, ProxiPlate™, PerkinElmer Life Sciences), and data were collected with a SpectraMax M5 plate reader from Molecular Devices equipped with SoftMax Pro software (version 5.4.5 for Macintosh OS X). Data were expressed as change in polarization (ΔPolarization) normalizing each individual replicate by the corresponding polarization value of fluorescein-labeled FGF2 in the absence of Tec kinase. The corresponding binding curve was used to calculate the dissociation constant with data fitting using the quadratic solution of the law of mass action,

$$y = P_0 + (P_{max} - P_0) \cdot \frac{\frac{x + L + K}{2} - \sqrt{\left(\frac{x + L + K}{2}\right)^2 - xL}}{L} \quad \text{(Eq. 1)}$$

where P_0 and P_m represent minimum and maximum values for the polarization, x is the Tec concentration, L is the concentration of labeled FGF2, and K is the dissociation constant. Fitting was performed using GraphPad Prism (version 5.0 for Macintosh OS X).

To establish a specific interaction between FGF2 and GST-NΔ173 Tec as well as the SH1 kinase domain of Tec, competition experiments with unlabeled FGF2 were performed (Fig. 2, *B* and *C*). Experiments were conducted at 50 nM fluorescein-labeled His-FGF2 in the presence and absence of 1.25 μM GST-NΔ173 Tec or the SH1 kinase domain under the conditions described above. In addition, conditions were varied based upon the presence or absence of an unlabeled FGF2 competitor molecule at 50 μM.

A Protein-Protein Interaction Assay Designed to Screen Small Molecule Libraries for Compounds Inhibiting FGF2 Binding to Tec Kinase (AlphaScreen® Assay)—To quantify the interaction of FGF2 with Tec kinase under screening conditions, an assay

was established based upon Alpha® technology (47). Briefly, this methodology is based on a pair of proteins of interest that bind to Alpha® donor and acceptor beads, respectively. Upon excitation of donor beads at 680 nm, singlet oxygen species are produced that can diffuse within a range of about 200 nm. If donor and acceptor beads are in close proximity due to the protein-protein interaction, singlet oxygen species will transfer energy to acceptor beads. This in turn causes emission of light with a wavelength of 520 nm that is detected as the Alpha® signal.

For all individual preparations and experiments of His-tagged FGF2 and GST-tagged NΔ173 Tec, optimal protein concentrations in AlphaScreen® assays were determined in cross-titration experiments. Typically, GST-tagged NΔ173 was used at a concentration of 30 nM, and His-tagged FGF2 was used in a range between 62.5 and 125 nM (data not shown). To quantify binding affinity between His-tagged FGF2 and GST-NΔ173 Tec and to assess the specificity of the Alpha® signal for their interaction, competition experiments were conducted with an untagged version of FGF2 (NΔ25-FGF2; Fig. 3). As specificity control for the competition by untagged FGF2, an Alpha® assay was conducted using an unrelated protein-protein interaction pair (GST-Titin/His-MBP-CARP) at a final concentration of 20 nM each. Briefly, after incubation of the proteins for 75 min at room temperature in PBS (supplemented with 0.1% BSA, 0.05% Tween 20), glutathione donor beads (catalog no. 6765300, PerkinElmer Life Sciences) and Ni-NTA acceptor beads (catalog no. 6760619, PerkinElmer Life Sciences) were added at a concentration of 7.5 μg/ml in a final volume of 15 μl. Following incubation for an additional 2 h, Alpha® protein interaction signals were recorded. All Alpha® assays were carried out in white low volume 384-well plates (catalog no. 6008280, ProxiPlate™) using an EnVision plate reader (PerkinElmer Life Sciences). The obtained data points were fitted with GraphPad Prism (version 5.0 for Macintosh OS X) using the cubic solution of the law of mass action for competitive binding of two ligands to one binding site (cubic equation (55)) to calculate the dissociation constant for the interaction between GST-NΔ173 Tec and His-tagged FGF2.

Screening of a Collection of Small Molecules for Inhibitors of the Interaction between FGF2 and Tec Kinase—AlphaScreen® experiments were performed as described above. GST-NΔ173 Tec (30 nM) and His-tagged FGF2 (125 nM) were combined in screening buffer (20 mM Tris-HCl, 150 mM NaCl, 1 mM DTT, 0.1% BSA, 0.05% Tween 20) and preincubated for 60 min in the presence of compounds or under mock control conditions (DMSO). Afterward, glutathione-coated donor and Ni-NTA-coated acceptor beads were added. Following 60 min of incubation, Alpha® signals were recorded using an EnVision™ plate reader (PerkinElmer Life Sciences). In the primary screen, 79,000 compounds of a scaffold-based library were tested at a final concentration of 40 μM. Reordered or synthesized compounds were tested in dose-response experiments using an 11-fold 1:1 serial dilution starting at 200 μM. The serially diluted compounds were also tested in a deselection assay with a non-related protein pair, GST-Titin and His-tagged MBP-CARP (20 nM each), to evaluate the specificity of compounds inhibiting the interaction of GST-NΔ173 Tec and His-tagged FGF2. Finally, GST-His-Biotin, a fusion protein containing both an N-terminal GST tag and a C-terminal His tag, was used at 20 nM as an additional technical control. To generate dose-response curves and corresponding IC_{50} values (Fig. 5; 13-fold 1:2 serial dilution starting at 200 μM), compounds were reordered from an independent batch of synthesis (compound 6, catalog no. *Z51196782*; compound 14, catalog no. *Z15516480*; compound 21, catalog no. *Z17100166*; compound 18, catalog no. *BJ01-04*; compound 19, catalog no. *BJ01-05* (all compounds from Enamine)). Compound powders were dissolved in DMSO with a stock concentration of 10 mM, incubated for 10 min at 37 °C, and further treated by sonication for 5 min at room temperature. Compound stock solutions were stored at −20 °C.

Biochemical Reconstitution of Tec Kinase-mediated Tyrosine Phosphorylation of FGF2 and STAP1 (Figs. 6 and 7)—A Tec kinase *in vitro* phosphorylation assay was established to test the inhibitory potential and selectivity of the small molecule inhibitors reported in this study (Figs. 6 and 7). Tyrosine phosphorylation of FGF2 and STAP1, another established substrate of Tec kinase (48, 49), was tested in a final volume of 100 μl (60 mM HEPES, pH 7.5, 3 mM $MgCl_2$, 20 μM ATP, 3 μM sodium orthovanadate, 1.2 mM DTT, 50 ng/μl PEG 20000, 0.05% (w/v) Tween 20, 0.001% BSA). GST-NΔ173Tec (60 nM) was incubated in the absence (1% DMSO mock control) or presence of each compound (50 μM in 1% DMSO). Where indicated, reactions contained a 250 nM concentration of either FGF2 or STAP1 (Hölzel Diagnostika, catalog no. GWB-P0486E-100). Following incubation at 30 °C for 45 min (corresponding to the midpoint of linear product formation), the reaction was terminated using SDS sample buffer and incubation for 4 min at 95 °C. Proteins were separated by SDS-PAGE (BisTris 4–12% acrylamide gradient) and transferred to PVDF membranes. Phosphorylation levels of GST-NΔ173 Tec (autophosphorylation), FGF2, and STAP1 were quantified by a Western analysis using affinity-purified, polyclonal anti-phosphotyrosine antibodies (rabbit) raised against a FGF2-derived synthetic peptide containing a phosphorylated tyrosine residue (ANRpYLAMKED, where pY represents phosphotyrosine). This antibody was found to recognize both tyrosine-phosphorylated FGF2 and autophosphorylated Tec kinase. Phosphorylation levels of STAP1 were monitored using a monoclonal anti-phosphotyrosine antibody (clone 4G10®, catalog no. 05-321, Merck Millipore). Appropriate fluorescent secondary antibodies (goat anti-rabbit IgG conjugated with Alexa Fluor® 680, catalog no. A-21076, Life Technologies, Inc.; goat anti-mouse IgG conjugated with Alexa Fluor® 680, catalog no. A-21057, Life Technologies) were used to quantify all antigens employing the LI-COR Odyssey infrared imaging platform. In Fig. 6*B*, an SDS gel corresponding to the Western analysis shown in Fig. 6*A* was stained with Coomassie InstantBlue (Expedeon) to control for protein amounts and purity. The PageRuler prestained protein ladder was used, containing marker proteins with the following molecular masses: 140, 115, 80, 65, 50, 40, 30, 25, 15, and 10 kDa (Thermo Scientific/Fermentas, catalog no. 26616).

Quantification of FGF2 Tyrosine Phosphorylation in Cells (Fig. 8)—CHO cells expressing FGF2-GFP in a doxycycline-dependent manner were incubated in the presence of active (compounds 6, 14, and 21) and inactive (compounds 18 and 19) com-

pounds (50 μM in 0.5% DMSO) as well as under mock conditions (0.5% DMSO). Incubation times were identical to those in experiments quantifying FGF2 secretion and cell viability (see below; Figs. 9 and 10). Cells were lysed in a detergent-containing buffer (50 mM Tris, pH 7.4, 150 mM NaCl, 1 mM EDTA, 1% (w/v) Nonidet P-40, 1 mM sodium vanadate, 0.1% 2-mercaptoethanol, 1× EDTA-free protease inhibitor mixture from Roche Applied Science, 1× phospho-stop mixture from Roche Applied Science). Following lysis using sonication, a clear supernatant was obtained by low speed centrifugation, removing aggregated material. GFP trap magnetic beads (Chromotek; GFP-Trap®_MA) were added to affinity-purify FGF2-GFP according to standard procedures. Beads were treated with SDS sample buffer followed by SDS-PAGE and Western blotting. Signals were quantified using the LI-COR imaging platform. Antigens were detected using anti-phosphotyrosine antibodies (4G10; Millipore) and affinity-purified anti-FGF2 antibodies (26, 50).

Quantification of FGF2 Secretion Using Cell Surface Biotinylation (Fig. 9)—Secreted FGF2 remains bound to heparan sulfates on cell surfaces without release into cell culture supernatants (8, 50). This allows for biochemical detection of the secreted population based upon cell surface biotinylation experiments (8, 23, 26, 51). CHO cells stably expressing FGF2-GFP in a doxycycline-dependent manner were cultivated in the presence of compounds 6, 14, 21, 18, and 19 (see Figs. 4 (58) and 5) at 10, 25, and 50 μM in 0.5% DMSO (final concentration) as well as under mock conditions. Following incubation at 37 °C for 24 h, in the continued presence of compounds, doxycycline was added to induce expression of FGF2-GFP. After another 16 h of cultivation at 37 °C, cells were treated with a membrane-impermeable biotinylation reagent, EZ-Link Sulfo-NHS-SS-Biotin (sulfosuccinimidyl-2-[biotinamido]ethyl-1,3-dithiopropionate, catalog no. 21331; Pierce), targeting primary amines on cell surface proteins. Following quenching and detergent-mediated cell lysis, biotinylated material and non-biotinylated material were separated from each other using streptavidin beads (UltraLink immobilized streptavidin, Pierce). Aliquots from the total cell lysate (corresponding to input) and aliquots of the purified biotinylated fractions (corresponding to the secreted population) were subjected to SDS-PAGE and Western analysis. Affinity-purified anti-GFP antibodies (50) and monoclonal anti-GAPDH antibodies (Lifetech-Ambion) were used to detect FGF2-GFP and GAPDH, respectively. GAPDH was used as a control protein localized exclusively to the intracellular space. Using appropriate fluorescent secondary antibodies, FGF2-GFP and GAPDH were quantified using the LI-COR Odyssey imaging platform. FGF2 secretion under mock conditions (0.5% DMSO) was defined as 100% secretion efficiency.

Quantitative Analysis of Cell Proliferation (Fig. 10)—To detect potential pleiotropic effects on cell viability of small molecule inhibitors, we monitored cell proliferation in the absence and presence of the compounds introduced in Fig. 4 (58). CHO cells constitutively expressing mCherry fused to a nuclear localization signal (56, 57) were cultivated under conditions equivalent to those in the experiments shown in Fig. 9. Cell proliferation was quantified in real time, employing an IncuCyte® Zoom live cell imaging microscope (Essen BioScience), providing an absolute quantification of fluorescent cell nuclei with kinetic resolution (34). In this way, cell proliferation was monitored for 72 h (with measurements conducted every 2 h) under the conditions indicated (Fig. 10).

Author Contributions—G. L. V., P. S., and S. W. performed the majority of the described experiments. H.-M. M. and J. P. S. contributed reagents and experimental work. M. G. generated, purified and characterized anti-phospho-FGF2 antibodies. E. D. conducted cell-based experiments in the presence of Tec/FGF2 inhibitors. N. H. and M. P. M. interpreted data from polarization experiments. U. U., D. W. W., and J. D. L. interpreted the chemistry of the identified compounds with regard to structure-activity relationships. W. N. contributed to the study design, interpreted all data, and wrote the manuscript.

Acknowledgments—We thank Siegfried Labeit (Department of Integrative Pathophysiology, Medical Faculty Mannheim, University of Heidelberg) for kindly providing preparations of GST-Titin and His-tagged MBP-CARP. The joint EMBL-DKFZ-University of Heidelberg Chemical Biology Core Facility is acknowledged for support in the small molecule screening process.

References

1. Nickel, W., and Seedorf, M. (2008) Unconventional mechanisms of protein transport to the cell surface of eukaryotic cells. *Annu. Rev. Cell Dev. Biol.* **24,** 287–308
2. Nickel, W., and Rabouille, C. (2009) Mechanisms of regulated unconventional protein secretion. *Nat. Rev. Mol. Cell Biol.* **10,** 148–155
3. Rabouille, C., Malhotra, V., and Nickel, W. (2012) Diversity in unconventional protein secretion. *J. Cell Sci.* **125,** 5251–5255
4. Malhotra, V. (2013) Unconventional protein secretion: an evolving mechanism. *EMBO J.* **32,** 1660–1664
5. Zhang, M., and Schekman, R. (2013) Cell biology. Unconventional secretion, unconventional solutions. *Science* **340,** 559–561
6. Rubartelli, A., Cozzolino, F., Talio, M., and Sitia, R. (1990) A novel secretory pathway for interleukin-1β, a protein lacking a signal sequence. *EMBO J.* **9,** 1503–1510
7. Florkiewicz, R. Z., Majack, R. A., Buechler, R. D., and Florkiewicz, E. (1995) Quantitative export of FGF-2 occurs through an alternative, energy-dependent, non-ER/Golgi pathway. *J. Cell Physiol.* **162,** 388–399
8. Trudel, C., Faure-Desire, V., Florkiewicz, R. Z., and Baird, A. (2000) Translocation of FGF2 to the cell surface without release into conditioned media. *J. Cell Physiol.* **185,** 260–268
9. Nickel, W. (2011) The unconventional secretory machinery of fibroblast growth factor 2. *Traffic* **12,** 799–805
10. Piccioli, P., and Rubartelli, A. (2013) The secretion of IL-1β and options for release. *Semin. Immunol.* **25,** 425–429
11. Steringer, J. P., Müller, H. M., and Nickel, W. (2015) Unconventional secretion of fibroblast growth factor 2: a novel type of protein translocation across membranes? *J. Mol. Biol.* **427,** 1202–1210
12. La Venuta, G., Zeitler, M., Steringer, J. P., Müller, H. M., and Nickel, W. (2015) The startling properties of fibroblast growth factor 2: how to exit mammalian cells without a signal peptide at hand. *J. Biol. Chem.* **290,** 27015–27020
13. Dupont, N., Jiang, S., Pilli, M., Ornatowski, W., Bhattacharya, D., and Deretic, V. (2011) Autophagy-based unconventional secretory pathway for extracellular delivery of IL-1β. *EMBO J.* **30,** 4701–4711
14. Deretic, V., Jiang, S., and Dupont, N. (2012) Autophagy intersections with conventional and unconventional secretion in tissue development, remodeling and inflammation. *Trends Cell Biol.* **22,** 397–406
15. Zhang, M., Kenny, S. J., Ge, L., Xu, K., and Schekman, R. (2015) Translo-

cation of interleukin-1β into a vesicle intermediate in autophagy-mediated secretion. *Elife* 10.7554/eLife.11205
16. Martin-Sánchez, F., Diamond, C., Zeitler, M., Gomez, A. I., Baroja-Mazo, A., Bagnall, J., Spiller, D., White, M., Daniels, M. J., Mortellaro, A., Peñalver, M., Paszek, P., Steringer, J. P., Nickel, W., Brough, D., and Pelegrín, P. (2016) Inflammasome-dependent IL-1β release depends upon membrane permeabilisation. *Cell Death Differ.* **23,** 1219–1231
17. Backhaus, R., Zehe, C., Wegehingel, S., Kehlenbach, A., Schwappach, B., and Nickel, W. (2004) Unconventional protein secretion: membrane translocation of FGF-2 does not require protein unfolding. *J. Cell Sci.* **117,** 1727–1736
18. Nickel, W. (2005) Unconventional secretory routes: direct protein export across the plasma membrane of mammalian cells. *Traffic* **6,** 607–614
19. Schäfer, T., Zentgraf, H., Zehe, C., Brügger, B., Bernhagen, J., and Nickel, W. (2004) Unconventional secretion of fibroblast growth factor 2 is mediated by direct translocation across the plasma membrane of mammalian cells. *J. Biol. Chem.* **279,** 6244–6251
20. Torrado, L. C., Temmerman, K., Müller, H. M., Mayer, M. P., Seelenmeyer, C., Backhaus, R., and Nickel, W. (2009) An intrinsic quality-control mechanism ensures unconventional secretion of fibroblast growth factor 2 in a folded conformation. *J. Cell Sci.* **122,** 3322–3329
21. Temmerman, K., Ebert, A. D., Müller, H. M., Sinning, I., Tews, I., and Nickel, W. (2008) A direct role for phosphatidylinositol 4,5-bisphosphate in unconventional secretion of fibroblast growth factor 2. *Traffic* **9,** 1204–1217
22. Temmerman, K., and Nickel, W. (2009) A novel flow cytometric assay to quantify interactions between proteins and membrane lipids. *J. Lipid Res.* **50,** 1245–1254
23. Müller, H. M., Steringer, J. P., Wegehingel, S., Bleicken, S., Münster, M., Dimou, E., Unger, S., Weidmann, G., Andreas, H., García-Sáez, A. J., Wild, K., Sinning, I., and Nickel, W. (2015) Formation of disulfide bridges drives oligomerization, membrane pore formation, and translocation of fibroblast growth factor 2 to cell surfaces. *J. Biol. Chem.* **290,** 8925–8937
24. Steringer, J. P., Bleicken, S., Andreas, H., Zacherl, S., Laussmann, M., Temmerman, K., Contreras, F. X., Bharat, T. A., Lechner, J., Müller, H. M., Briggs, J. A., García-Sáez, A. J., and Nickel, W. (2012) Phosphatidylinositol 4,5-bisphosphate ($PI(4,5)P_2$)-dependent oligomerization of fibroblast growth factor 2 (FGF2) triggers the formation of a lipidic membrane pore implicated in unconventional secretion. *J. Biol. Chem.* **287,** 27659–27669
25. Nickel, W. (2007) Unconventional secretion: an extracellular trap for export of fibroblast growth factor 2. *J. Cell Sci.* **120,** 2295–2299
26. Zehe, C., Engling, A., Wegehingel, S., Schäfer, T., and Nickel, W. (2006) Cell-surface heparan sulfate proteoglycans are essential components of the unconventional export machinery of FGF-2. *Proc. Natl. Acad. Sci. U.S.A.* **103,** 15479–15484
27. Debaisieux, S., Rayne, F., Yezid, H., and Beaumelle, B. (2012) The ins and outs of HIV-1 Tat. *Traffic* **13,** 355–363
28. Rayne, F., Debaisieux, S., Bonhoure, A., and Beaumelle, B. (2010) HIV-1 Tat is unconventionally secreted through the plasma membrane. *Cell Biol. Int.* **34,** 409–413
29. Rayne, F., Debaisieux, S., Yezid, H., Lin, Y. L., Mettling, C., Konate, K., Chazal, N., Arold, S. T., Pugnière, M., Sanchez, F., Bonhoure, A., Briant, L., Loret, E., Roy, C., and Beaumelle, B. (2010) Phosphatidylinositol-(4,5)-bisphosphate enables efficient secretion of HIV-1 Tat by infected T-cells. *EMBO J.* **29,** 1348–1362
30. Zeitler, M., Steringer, J. P., Müller, H. M., Mayer, M. P., and Nickel, W. (2015) HIV-Tat protein forms phosphoinositide-dependent membrane pores implicated in unconventional protein secretion. *J. Biol. Chem.* **290,** 21976–21984
31. Ebert, A. D., Laussmann, M., Wegehingel, S., Kaderali, L., Erfle, H., Reichert, J., Lechner, J., Beer, H. D., Pepperkok, R., and Nickel, W. (2010) Tec-kinase-mediated phosphorylation of fibroblast growth factor 2 is essential for unconventional secretion. *Traffic* **11,** 813–826
32. Florkiewicz, R. Z., Anchin, J., and Baird, A. (1998) The inhibition of fibroblast growth factor-2 export by cardenolides implies a novel function for the catalytic subunit of Na^+,K^+-ATPase. *J. Biol. Chem.* **273,** 544–551
33. Dahl, J. P., Binda, A., Canfield, V. A., and Levenson, R. (2000) Participation of Na,K-ATPase in FGF-2 secretion: rescue of ouabain-inhibitable FGF-2 secretion by ouabain-resistant Na,K-ATPase α subunits. *Biochemistry* **39,** 14877–14883
34. Zacherl, S., La Venuta, G., Müller, H. M., Wegehingel, S., Dimou, E., Sehr, P., Lewis, J. D., Erfle, H., Pepperkok, R., and Nickel, W. (2015) A direct role for ATP1A1 in unconventional secretion of fibroblast growth factor 2. *J. Biol. Chem.* **290,** 3654–3665
35. Kaplan, J. H. (2002) Biochemistry of Na,K-ATPase. *Annu. Rev. Biochem.* **71,** 511–535
36. Lewis, C. M., Broussard, C., Czar, M. J., and Schwartzberg, P. L. (2001) Tec kinases: modulators of lymphocyte signaling and development. *Curr. Opin. Immunol.* **13,** 317–325
37. Takesono, A., Finkelstein, L. D., and Schwartzberg, P. L. (2002) Beyond calcium: new signaling pathways for Tec family kinases. *J. Cell Sci.* **115,** 3039–3048
38. Mano, H. (1999) Tec family of protein-tyrosine kinases: an overview of their structure and function. *Cytokine Growth Factor Rev.* **10,** 267–280
39. Bradshaw, J. M. (2010) The Src, Syk, and Tec family kinases: distinct types of molecular switches. *Cell. Signal.* **22,** 1175–1184
40. Liu, P., Cheng, H., Roberts, T. M., and Zhao, J. J. (2009) Targeting the phosphoinositide 3-kinase pathway in cancer. *Nat. Rev. Drug Discov.* **8,** 627–644
41. Bikfalvi, A., Klein, S., Pintucci, G., and Rifkin, D. B. (1997) Biological roles of fibroblast growth factor-2. *Endocr. Rev.* **18,** 26–45
42. Presta, M., Dell'Era, P., Mitola, S., Moroni, E., Ronca, R., and Rusnati, M. (2005) Fibroblast growth factor/fibroblast growth factor receptor system in angiogenesis. *Cytokine Growth Factor Rev.* **16,** 159–178
43. Beenken, A., and Mohammadi, M. (2009) The FGF family: biology, pathophysiology and therapy. *Nat. Rev. Drug Discov.* **8,** 235–253
44. Nguyen, M., Watanabe, H., Budson, A. E., Richie, J. P., Hayes, D. F., and Folkman, J. (1994) Elevated levels of an angiogenic peptide, basic fibroblast growth factor, in the urine of patients with a wide spectrum of cancers. *J. Natl. Cancer Inst.* **86,** 356–361
45. Pardo, O. E., Latigo, J., Jeffery, R. E., Nye, E., Poulsom, R., Spencer-Dene, B., Lemoine, N. R., Stamp, G. W., Aboagye, E. O., and Seckl, M. J. (2009) The fibroblast growth factor receptor inhibitor PD173074 blocks small cell lung cancer growth *in vitro* and *in vivo*. *Cancer Res.* **69,** 8645–8651
46. Pardo, O. E., Wellbrock, C., Khanzada, U. K., Aubert, M., Arozarena, I., Davidson, S., Bowen, F., Parker, P. J., Filonenko, V. V., Gout, I. T., Sebire, N., Marais, R., Downward, J., and Seckl, M. J. (2006) FGF-2 protects small cell lung cancer cells from apoptosis through a complex involving PKCϵ, B-Raf and S6K2. *EMBO J.* **25,** 3078–3088
47. Taouji, S., Dahan, S., Bossé, R., and Chevet, E. (2009) Current screens based on the AlphaScreen technology for deciphering cell signalling pathways. *Curr. Genomics* **10,** 93–101
48. Ohya, K., Kajigaya, S., Kitanaka, A., Yoshida, K., Miyazato, A., Yamashita, Y., Yamanaka, T., Ikeda, U., Shimada, K., Ozawa, K., and Mano, H. (1999) Molecular cloning of a docking protein, BRDG1, that acts downstream of the Tec tyrosine kinase. *Proc. Natl. Acad. Sci. U.S.A.* **96,** 11976–11981
49. Yokohari, K., Yamashita, Y., Okada, S., Ohya, K., Oda, S., Hatano, M., Mano, H., Hirasawa, H., and Tokuhisa, T. (2001) Isoform-dependent interaction of BRDG1 with Tec kinase. *Biochem. Biophys. Res. Commun.* **289,** 414–420
50. Engling, A., Backhaus, R., Stegmayer, C., Zehe, C., Seelenmeyer, C., Kehlenbach, A., Schwappach, B., Wegehingel, S., and Nickel, W. (2002) Biosynthetic FGF-2 is targeted to non-lipid raft microdomains following translocation to the extracellular surface of CHO cells. *J. Cell Sci.* **115,** 3619–3631
51. Seelenmeyer, C., Wegehingel, S., Tews, I., Künzler, M., Aebi, M., and Nickel, W. (2005) Cell surface counter receptors are essential components of the unconventional export machinery of galectin-1. *J. Cell Biol.* **171,** 373–381
52. Scharenberg, A. M., and Kinet, J. P. (1998) PtdIns-3,4,5-P_3: a regulatory nexus between tyrosine kinases and sustained calcium signals. *Cell* **94,** 5–8
53. Contreras-Gómez, A., Sánchez-Mirón, A., García-Camacho, F., Molina-Grima, E., and Chisti, Y. (2014) Protein production using the baculovirus-insect cell expression system. *Biotechnol. Prog.* **30,** 1–18

54. Jameson, D. M., and Seifried, S. E. (1999) Quantification of protein-protein interactions using fluorescence polarization. *Methods* **19,** 222–233
55. Thrall, S. H., Reinstein, J., Wöhrl, B. M., and Goody, R. S. (1996) Evaluation of human immunodeficiency virus type 1 reverse transcriptase primer tRNA binding by fluorescence spectroscopy: specificity and comparison to primer/template binding. *Biochemistry* **35,** 4609–4618
56. Kalderon, D., Roberts, B. L., Richardson, W. D., and Smith, A. E. (1984) A short amino acid sequence able to specify nuclear location. *Cell* **39,** 499–509
57. Fischer-Fantuzzi, L., and Vesco, C. (1988) Cell-dependent efficiency of reiterated nuclear signals in a mutant simian virus 40 oncoprotein targeted to the nucleus. *Mol. Cell Biol.* **8,** 5495–5503
58. Nickel, W., and Lewis, J. D. (March 29, 2016) Patent GB1605173.2